"SYNTHESIS OF GRAPHENE FOR EMI SHIELDING APPLICATION"

A Major Project Report submitted in the partial fulfillment for the Award of the Degree of

MASTER OF TECHNOLOGY

In

POLYMER TECHNOLOGY

Submitted by

MUKESH KUMAR PRAJAPATI
2K11/PTE/04

Under the Joint Supervision of

DR. RICHA SRIVASTAVA
Assistant Professor
Department of Applied Chemistry
& Polymer Technology
Delhi Technological University
New Delhi-110042

DR. PARVEEN SAINI
Scientist
Polymeric and Soft Materials Section,
Materials Physics & Engg. Division
CSIR-National Physical Laboratory
New Delhi-110012

Department of Applied Chemistry and Polymer Technology
Delhi Technological University, Delhi-110042

DECLARATION

*I **Mukesh Kumar Prajapati** hereby declares that the thesis entitled **"Synthesis Of Graphene For EMI Shielding Application"** is an authentic record of research work done by me under the supervision of **Dr. Praveen Saini, Scientist ,** Polymeric and Soft Material Section, CSIR-National Physical Laboratory and **Dr.Richa Srivastava, Assistant Professor** Delhi Technological University. This work has not been previously submitted for the award of any degree or diploma of this or any other University/Institute.*

Date **Mukesh Kumar Prajapati**

CERTIFICATE

This is to certify that the project report entitled "**SYNTHESIS OF GRAPHENE FOR EMI SHIELDING APPLICATION"** submitted by ***Mukesh Kumar Prajapati (2K11/PTE/04)*** in partial fulfillment for the award of degree of Master of Technology in Polymer Technology to Delhi Technological University, Delhi, is a record of the work carried out by him under our supervision. The work has been carried out from 8th January, 2013 to 8th July, 2013. The project embodies the original work done by him to the best of our knowledge and has not been submitted to any other degree of this or any other university. The matter embodied in this project report is original and not copied from any source without proper citation.

Dr. Richa Srivastava
Assistant Professor
Department of Applied Chemistry
& Polymer Technology
Delhi Technological University
New Delhi-110042

Dr. Parveen Saini
Scientist
Polymeric and Soft Material Section
Materials Physics & Engg. Division
CSIR-National Physical Laboratory
New Delhi 110012

Prof. (Dr.) D. Kumar
HOD
Department of Applied Chemistry
& Polymer Technology
Delhi Technological University
New Delhi-110042

Dr. Rajeev Chopra
Head
Human Resource Development
CSIR-National Physical Laboratory
New Delhi 110012

ACKNOWLEDGEMENT

First of all I would like to thank ***Prof. (Dr.) D. Kumar, Head,*** *Department of Applied Chemistry and Polymer Technology, Delhi Technological University (DTU), for allowing me to carry out this project work at NPL.*

I wish to express my sincere thanks to Prof. R. C. Budhani, Director, CSIR- NPL, Dr. Rajiv Chopra, Head, HRD Group and Dr. A. M. Biradar, Head, Polymeric and Soft Material Section for permitting and providing the facilities to carry out this thesis work.

I want to express my deep sense of gratitude to my supervisors ***Dr. Parveen Saini, CSIR-NPL*** *and* ***Dr. Richa Srivastava, DTU*** *for guidance and encouragement which has been a great source of inspiration to me. Their constant suggestions and cooperation have been invaluable and I was greatly benefited by their vast knowledge and practical experience.*

I am grateful to Dr. Manju Arora, CSIR-NPL for her invaluable guidance, support and motivation in my research work.

My special thanks to Dr. K. K. Saini, for extending lab facilities and for giving useful tips.

I am highly thankful to Prof. G. L. Verma, Prof. A. P. Gupta, Prof. R. C. Sharma, Dr. Archana Rani, Dr. Ram Singh, Dr. Saurabh Mehta, Dr. Anil Kumar, Dr. D. Santhiya, Dr. Roli Purwar Dr. Raminder Kaur, and Mr. S. G. Warkar for their guidance and support.

I would also like to thank Ms. Chandni Puri, CSIR- NPL for useful discussions and support in material synthesis. Special thanks to Mr. Gautam Ahuja, Mr. Mukesh Gocher and Mr. Sandeep Tripathi for their co-operation and for extending all possible help during the course of my experiments. I am also thankful to all my classmates for their invaluable suggestions and support throughout my M. Tech.

I am even more indebted to ***my parents*** *for their inspiration, love, care, patience, sacrifices and support.*

Mukesh Kumar Prajapati

INDEX

LIST OF FIGURES

LIST OF TABLES

ABSTRACT

Graphite oxide (GO) has been synthesized from graphite by chemical oxidation method and characterized for its thermal, morphological and structural attributes by techniques such as thermogravimetric analysis (TGA), high resolution transmission electron microscopy (HRTEM), Raman, Fourier transform infrared (FTIR) spectroscopy, and powder X-ray diffraction (XRD). The as synthesized GO was used to prepare graphene coated cotton-polyester fabric by dip coating technique followed by chemical reduction. These fabrics were subjected to SEM, XRD, TGA and contact angle measurements which confirm the presence of GO coating over fabrics and its successful conversion into reduced GO (RGO) after chemical reduction. It was also observed that increase in graphene loading leads to enhancement of both electrical conductivity and mechanical properties. Interestingly, the low conductivity samples (graphene loading <2%) conforms to anti-static resistance range whereas higher graphene loading sample (>7 %) display electromagnetic interference (EMI) shielding capability with shielding effectiveness value upto -26.67 dB for a three layer shield.

CHAPTER 1

INTRODUCTION

Information and communications technology has witnessed rapid growth especially after the arrival of wireless technology. Electromagnetic (EM) waves with ultra high frequencies (300 MHz-3 GHz) and super high frequencies (3-30 GHz) are often used to transfer a great amount of information at high speeds. In practice, such EM waves have already been applied to cordless phones (0.8-2 GHz), wireless local area network (2.45-5.2 GHz), electronic toll collection (5.8 GHz), microwave devices/communications, communication satellites, satellite television broadcasting (90-140 GHz) etc. In the near future, EM waves with extremely high frequencies will be required for high speed communications and the spread of intelligent transportation system.

The proliferation of electronics and widespread instrumentation has generated EM interference (EMI) as an offshoot. In a true sense, EMI is a novel kind of pollution which tries to interrupt the usual functioning of electronic appliances or may also lead to complete disruption of a gadget's performance. The consequent hazards may be loss of revenue, energy, time, or even precious human life. Therefore, some blocking mechanism must be provided to isolate the internals of an appliance from the surroundings, i.e., to limit the amount of EMI radiation from the external environment that can penetrate the circuit or conversely to regulate the electromagnetic (EM) energy generated by the circuit that can escape into the external environment of radio frequency radiation continues to be a more serious concern in this modern society **[1].** More generally prevention of the propagation of electric and magnetic waves from one region to another by using conducting or magnetic materials is defined as electromagnetic shielding. Three mechanisms are given for EMI shielding i.e. primary, secondary, and tertiary. The primary mechanism of shielding is reflection and the material used for shielding by reflection requires mobile charge carrier like electron or hole i.e. shield used should have conducting property. Metals are most common shield material which uses reflection mechanism for shielding as they have free charge carriers. Since metal (sheets) are bulky so cannot be used as such. For translating shielding property of metals, they are coated on insulating surfaces. Metal coatings are generally made by electroplating, electroless plating or vacuum deposition on bulk materials, fibers or particles. Metal having good shielding property suffers problems like poor wear resistance, low scratch resistance, high weight, corrosion susceptibility and high cost [2]. The secondary

mechanism is absorption for which shield material should have electrical or magnetic dipole. For such a purpose materials with high dielectric constant like ZnO, SiO_2, TiO_2, $BaTiO_3$, or high magnetic permeability e.g. carbonyl iron, Ni, Co, or Fe metals, γ-Fe_2O_3, Fe_3O_4, etc are used. However, these materials or their composites possess problems like low permittivity or permeability at gigahertz frequencies, weight penalties, narrow-band action, and processing difficulties. Other than reflection and absorption, a mechanism of shielding is multiple reflections, which refer to the reflections at various surfaces or interfaces in the shield. This mechanism requires the presence of a large surface area or interface area in the shield. An example of a shield with a large surface area is a porous material. Other use of a shield with a large interface area is a conducting composite material containing filler which has a large surface area [3]. For such a purpose, electrically conducting polymer composites have gained recent popularity because of their light weight, resistance to corrosion, flexibility, and processing advantages in particular, polymer composites conducting additives like metal particles, fibers or whiskers, carbon black, graphite powder or carbon nanotubes. However the functioning of antistatic agents is critically dependent on the relative humidity whereas the metal and carbon filled materials suffered from the problems like bleeding, poor dispersion and irreproducible results. In addition to filled composites, surface coating of metals done by electroplating, electroless plating or vacuum deposition techniques, tend to suffer from their poor wear or scratch resistance. For a given conducting composition, electrical conductivity is determined by the amount, type and shape of the conducting filler. For example spherical filler like carbon black (CB) loaded antistatic compositions usually contain >10 % CB which often exert a negative influence on the processability and mechanical properties of the material. In contrast, although the high aspect ratio filler like carbon nanotubes, shows antistatic action even at loading of 0.3 wt %, but the dispersion remains a big problem. Graphene has emerged as new conducting material for various applications due to its outstanding mechanical, thermal, optical, electronic, excitonic properties and ability to be manipulated via chemical route [4-7].

Recently electrically conductive textiles have been of increasing research interest due to their numerous possibilities for application in various fields of activity. Conductive fabrics represent potential application in clothing as well as in the medical and military fields, as sensors, actuators, electromagnetic shields, anti static dissipative etc. Recent advances in material science and nanotechnology with the combination of unique properties of fibers has caused the emergence of advanced textiles [8]. The creation of electrical conductivity feature to the textile substrates is an essential key for the fabrication of such advanced fibrous

materials. Electroconductive textiles can be made using metal strands or metallic fibers mixed with textile fibers woven into the construction of the textile. However, because both metals and classical semiconductor are stiff material, they are not very suitable for textile fiber applications since fibers are subjected to a high degree of stretch and bending during their application [9]. Also Conductivity has been provided by various materials such as conjugated polymers like carbon nanotubes, polyaniline, But, the most widly used methods require complex processes, expensive materials and pre-functionalization have some disadvantages such as lacking uniform coating, flexibility, and durable wear-resistance, which also increases the cost of production. Nanoscale materials based on 2-D graphene sheets have attracted much attention recently due to many unusual and novel properties predicted. Graphene with high electrical conductivity can serve as new nanoscale building blocks to create unique electroconductive materials which can be better used for anti static dissipation and EMI shielding application [10-12].

1.1 Research Objective

Graphene is an emerging material with unique electrical, thermal and mechanical properties and wide range of applications. However, realization of remarkable properties of individual graphene sheets into advanced, macroscopic, functional structures for practical applications; require an effective assembly strategy with strict control over above properties. Therefore, for translation of graphene's properties into product it has to be transformed into suitable form including, graphene papers, transparent/conducting films, graphene fiber or 3D framework and graphene nanocomposite materials. In this project work, my research objective is to synthesise graphene and to use its conducting property for EMI shielding application by synthesising graphene coated fabrics.

- Synthesis of graphite oxide and its coating on fabric surface followed by chemical reduction to obtain graphene coated fabric.
- Optimizing the conditions for obtaining the graphene with best combination of surface area and electrical properties.
- Characterization of graphite oxide and graphene coated fabric by XRD, SEM, HRTEM, TGA, FTIR, Raman, contact angle, mechanical strength and conductivity measurement techniques.
- To use reduced graphene oxide coated fabrics based microwave shields.
- Evaluation of their EMI shielding performance.

1.2 Organization of Thesis

Chapter 1 (Introduction) provides the brief overview of the research background including definition of problem.

Chapter 2 (Literature Review) provide information about carbon materials, graphene history, synthesis and property, electroconducting fabric uses and applications.

Chapter 3 (Materials and Methods) describes in detail all the materials and equipments used in the present study. This is followed by the experimental procedure which includes synthesis of graphene and its coating on fabric surface and details of experimental techniques and parameters.

Chapter 4 (Results and Discussion) In this chapter results of different characterization and their discussions are given.

Chapter 6 (Conclusion) provides major finding in this research work.

CHAPTER 2

LITERATURE REVIEW

Until the 1980s, the carbon family was limited to the well-known materials graphite and diamond. This has totally changed with the discovery of other carbon allotropes viz. fullerenes, CNTs and very recently graphene. Among these carbonaceous materials, graphene has attracted tremendous research interest due to its unique structural features and outstanding properties [10]. Graphene has demonstrated a variety of intriguing properties including high electron mobility at room temperature (250,000 cm^2/Vs), exceptional thermal conductivity (5000Wm^{-1} K^{-1}), superior mechanical properties (Young's modulus of ~1 TPa and intrinsic strength of ~130 GPa), complete impermeability to any gases, ability to sustain extremely high densities of electric current (a million times higher than copper) and easy chemical functionalization comparative to other materials (Table-1)[13-14]. Moreover, the production cost of graphene is very low in comparison to other carbon-based nanomaterials.

Table1: Properties of graphene, CNT, nano sized steel, and polymers.

Materials	Tensile strength (GPa)	Thermal conductivity (W/mK)	Electrical conductivity (S/m)
Graphene	**130±10**	**$(4.84\pm0.44)\times10^3$ to $(5.30\pm0.48)\times10^3$**	**7200**
CNT	**60-150**	**3500**	**3000-4000**
Nano sized steel	**1769**	**5-6**	**1.35×10^6**
Plastic (HDPE)	**0.018-0.020**	**0.46-0.52**	**Insulator**
Rubber (Natural)	**0.02-0.03**	**0.13-0.142**	**Insulator**
Fiber (Kevlar)	**3.62**	**0.04**	**Insulator**

.

Despite having similar carbon-carbon network as other carbon materials, the different molecular architecture is responsible for wide differences in their properties. Therefore, for

better understanding of graphene, its properties and relative advantages, a brief introduction of carbon and its allotropes is extremely important.

2.1 BACKGROUND OF CARBON MATERIALS

Initially carbon was discovered as charcoal by A.L. Lavoisier in 1789. It is widely distributed in nature with coal as its main source. Carbon has four electrons in four hybridized bonding orbital ($2s^1 2px^1 2py^1 2pz^1$) that are available to form covalent chemical bonds. It develops into different allotropes viz. diamond, graphite, fullerenes, carbon nanotubes and more lately graphene. These allotropes display a variety of interesting structural and electronic properties due to coexistence of sp^2 and sp^3 hybridized carbon atoms in different proportions.

2.2 DIAMOND

Diamond is an allotrope of carbon with sp^3 hybridized orbitals that arranged in 3d space to form tetrahedral structure. Due to strong covalent bonding, diamond is hardest known material. All the orbital in diamond are filled with no free electron in valance shell that makes diamond an insulating material with wide band gap. Due to its unparalled hardness, most applications of diamond are related to industrial purpose like grinding drilling, polishing and cutting [15]. Besides, its suitable refractive index, high optical dispersion and ability to cut along various crystal planes gives diamond its characteristic lustre making it precious gemstone for jewellery and adornments.

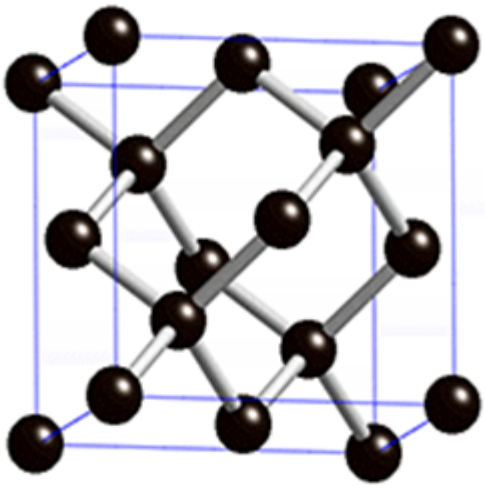

Fig 1: Structure of diamond.

2.3 GRAPHITE

Graphite is a soft material where carbon atoms are bonded trigonally with three carbon atoms in a plane. Such type of bonding makes the structure to assume a two dimensional layer type architecture having sp^2 hybridisation. However, due to intermolecular interactions, these layers stack over each other, to form 3D graphitic structure. These layers are bonded by weak Vander Walls forces responsible for softness of graphite and its lubrication properties. The delocalisation of one of the outer electrons of each atom forms a π-cloud which makes graphite an electrical conductor. The interlayer distance between layers is found to be 3.34 Å, with ABAB…. stacking sequence. Graphite has wide range of applications in the field of technology especially as a semiconducting material with a narrow band gap [16].

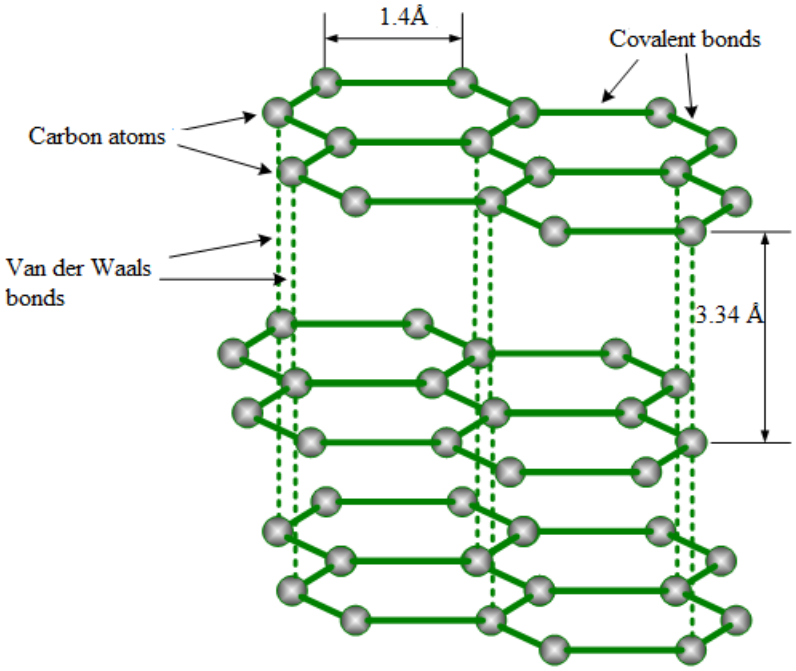

Fig 2: Structure of graphite

2.4 FULLERENE

A fullerene is any molecule composed entirely of carbon in the form of hollow sphere, ellipsoid or tube. Spherical fullerenes are also called buckyballs whereas cylindrical ones are called as carbon nanotube or buckytubes. Fullerenes are similar in structure to graphite which is composed of stacked graphene sheets of linked hexagonal ring, but they may also contain pentagonal or sometimes heptagonal rings. Buckyballs have been the subject of intense research, both for their unique chemistry and for their technological applications, especially

in materials science, electronics, and nanotechnology e.g. as electron acceptor in photovoltaic, for making inclusion compounds, quantum mechanics studies, superconductivity and anti-tumour research [17].

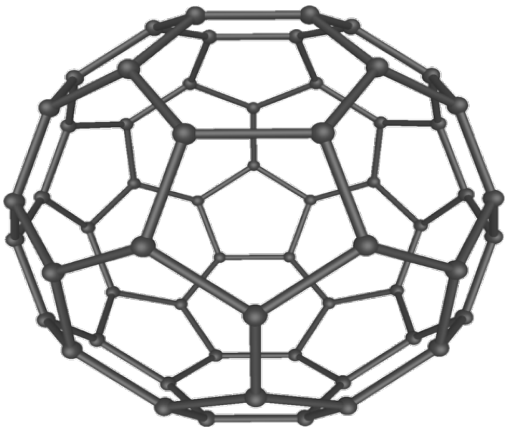

Fig 3: Structure of fullerene.

2.5 CARBON NANOTUBES

Carbon nanotubes (CNTs) are allotropes of carbon with a cylindrical nanostructure. Nanotubes have been constructed with length-to-diameter ratio of up to 132,000,000:1, significantly larger than for any other material. Owing to their extraordinary thermal conductivity and mechanical and electrical properties, carbon nanotubes find applications as additives to various structural materials. For instance, nanotubes form a tiny portion of the material(s) in some (primarily carbon fiber) baseball bats, golf clubs, or car parts. Nanotubes are members of the fullerene structural family. Their name is derived from their long, hollow structure with the walls formed by one-atom-thick sheets of carbon, called graphene. These sheets are rolled at specific and discrete angles, and the combination of the rolling angle and radius decides the nanotube properties; for example, whether the individual nanotube shell is a metal or semiconductor. Nanotubes are categorized as single-walled nanotubes (SWNTs) and multi-walled nanotubes (MWNTs). Individual nanotubes naturally align themselves into "ropes" held together by Van der Waals forces, more specifically, pi-stacking. These tubes of carbon are usually only a few nanometres wide (typically 1-2 nm for SWCNT and 2-25 nm for MWCNT), but they can range from less than a micrometer to several millimeters in length. They often have closed ends, but can be open-ended as well. Applied quantum chemistry, specifically, orbital hybridization best describes chemical bonding in nanotubes. The chemical bonding of nanotubes is composed entirely of sp^2 bonds, similar to those of

graphite. These bonds, which are stronger than the sp^3 bonds found in alkanes and diamond, provide nanotubes with their unique strength. and extraordinary macroscopic properties, including high tensile strength (100 GPa), high electrical conductivity (~$10^9 Acm^{-2}$), high ductility, high heat conductivity, and relative reactive inactivity as it is cylindrical and "planar" i.e. it has no "exposed" atoms that can be easily displaced [18-19].

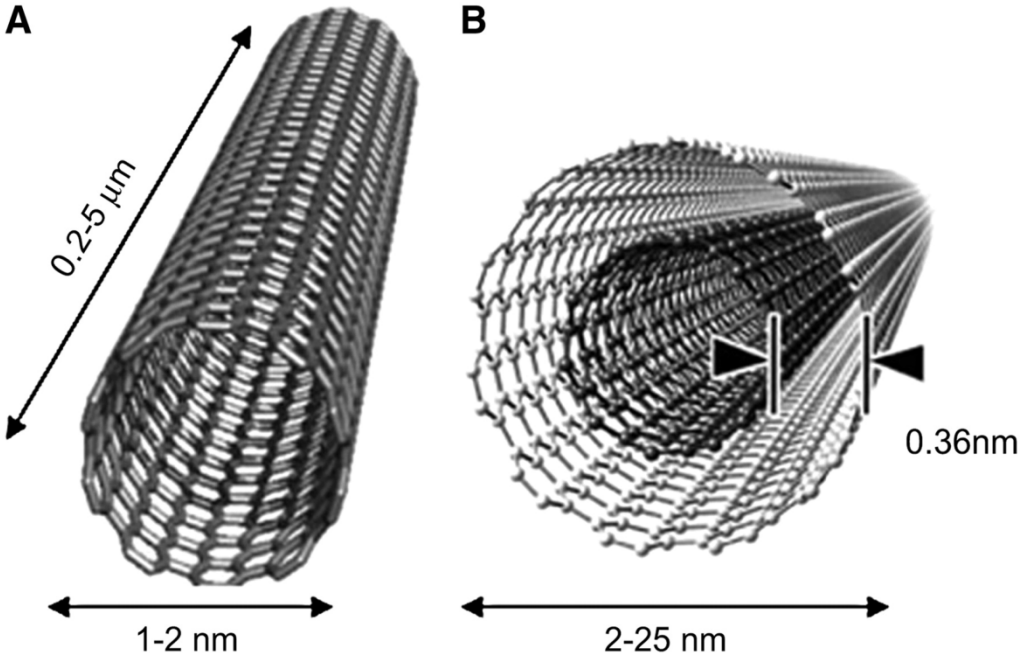

Fig 4: Structure of (a) singlewall and (b) multiwall carbon nanotubes.

2.6 GRAPHENE

The term graphene first appeared in 1987 to describe single sheets of graphite as one of the constituents of graphite intercalation compounds (GIC). Conceptually a GIC is a crystalline salt of the intercalant and graphene. The term was also used in early descriptions of carbon nanotubes as well as for epitaxial graphene. Single layers of graphite were previously (starting from the 1970s) grown epitaxially on top of other materials. This "epitaxial graphene" consists of a single-atom-thick hexagonal lattice of sp^2 bonded carbon atoms, as in free standing graphene. Single layer of graphite were also observed by transmission electron microscopy within bulk materials. The earliest TEM images of few-layer graphene were published by G. Ruess and F. Vogt in 1948. There have also been number of attempts to produce very thin film of graphite starting from 1990 and continuing until after 2004, by the method of mechanical and chemical exfoliation [20]

In 2004, Andre Geim and Kostya Novoselov extracted single-atom-thick crystallites (graphene) from bulk graphite and transferred them onto thin SiO_2 on a silicon wafer in a process sometimes called micromechanical cleavage or scotch tape method and were awarded 2010 physics noble prize for their pioneering work on graphene including estimation of mobility and unfolding anomalous quantum hall effect [21].

2.7. STRUCTURE OF GRAPHENE

Graphene is a one-atom-thick planar sheet of sp^2-bonded carbon atoms densely packed in a honeycomb crystal lattice. In a two-dimensional carbon system for graphene, three carbon electrons from four hybridized bonding electrons form strong in-plane sp^2 bonds consisting of a honeycomb structure, and a fourth electron spreads out over the top or bottom of the layer as a π electron. The term 'graphene' is commonly prefixed by 'monolayer', 'bilayer' or 'few-layar (<10 layers). Monolayer graphene is generally accepted to exists in a rippled form with no stacking of sheets, while few-layer graphene can have a number of stacking arrangements, including ABAB (Bernal stacking), ABCABC (rhombohedral stacking). Few-layer graphene with no discernible stacking order is also common and is termed as 'turbostratic.

Graphene is the basic structural element of some carbon allotropes including graphite, carbon nanotubes and fullerenes. It is the basic building block for graphitic materials of all other dimensionalities. By rolling it in one dimension it becomes a carbon nanotubes, stacking of one graphene layer on other three dimensional graphite structure is obtained while wrapping graphene zero dimensional fullerenes is obtained (figure 5) [21-22].

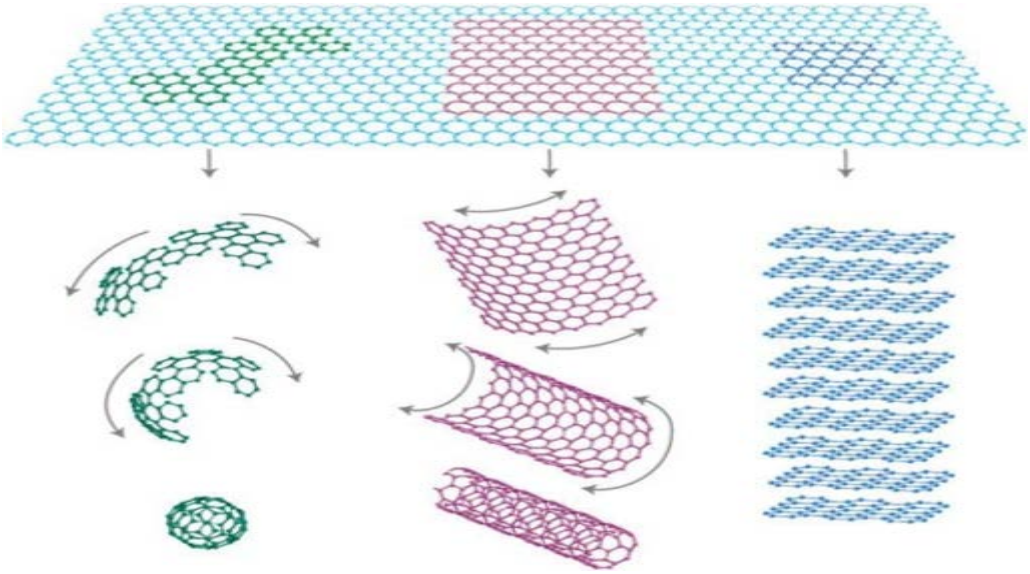

Fig 5: Graphene and its relation to fullerene, CNT and graphite.

2.8 SYNTHESIS OF GRAPHENE

As with any other nanomaterial, graphene too can be synthesized by top-down or bottom-up approach. Top-down routes involve breaking apart the stacked layers of graphite to yield single graphene sheets whereas bottom-up methods involve synthesising graphene from alternative carbon containing sources. For top-down methods, separating the stacked sheets means that the Van der Waals forces that hold the layers together must be overcome, which is not a trivial task despite the relatively low interlayer bonding energy. Key challenges in this area include effectively separating the layers without damaging the sheets, and preventing reagglomeration of the sheets once the layers have been exfoliated. Top-down approaches generally suffer from low yields, numerous steps, and have the common disadvantage that natural graphite is a finite resource and requires mining and processing prior to use. Graphite can be produced synthetically under high temperature conditions, but it is not generally suitable for graphene production due to poor levels of graphitisation and irregular morphologies. For bottom-up methods, high levels of graphitisation must be promoted to produce good quality material, so these methods generally require high temperatures. The processes involved are usually simple although the material produced can contain higher levels of defects than observed for top-down methods. In addition to forming graphene nanosheets, bottom-up methods can also be used to form large area graphene films via growth on certain substrates Figure:6 [23-24].

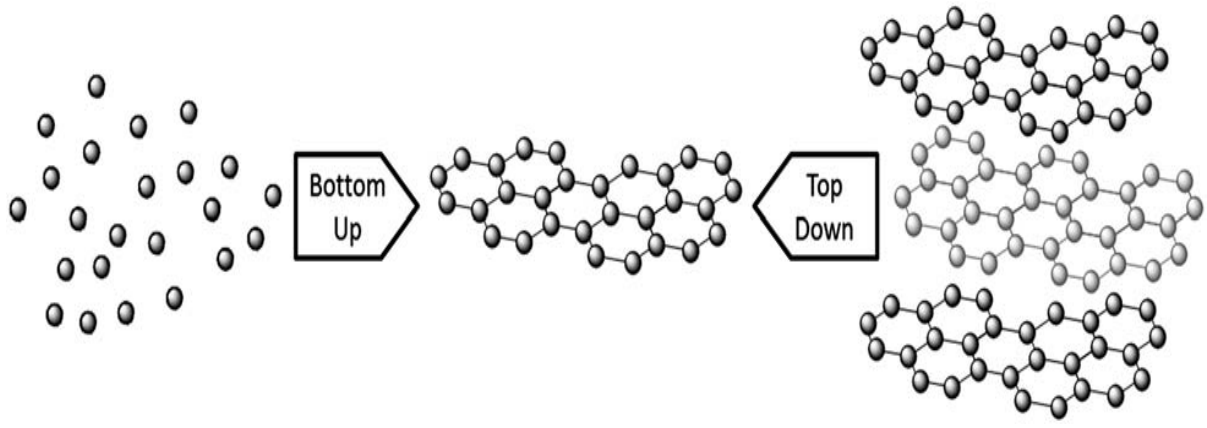

Fig 6: Top-down and bottom-up approach for graphene synthesis.

2.8.1 TOP-DOWN METHODS

2.8.1.1 EXFOLIATION OF GRAPHITE INTERCALATION COMPOUNDS (GIC)

Graphite intercalated compounds have been reported in 1940 by German scientist Schafhaeut involving intercalation and exfoliation of graphite using H_2SO_4 and HNO_3. Intercalation is insertion of a small-molecule or species such as an acid or alkali metal, in between the carbon lamellae. A number of intercalants have been tried in the past like alkali metals, fluoride salts of various type transition metals iron nickel and other organic species. Insertion of these intercalates widens spacing between stacked layers and exfoliation of these intercalated graphite compounds produces graphene layers. Number of strategies have been used for exfoliation of GICs like solvent assisted sonication or thermal exfoliation involving rapid heating (e.g microwave irradiation) [24-25].

2.8.1.2 ELECTROCHEMICAL EXFOLIATION

Electrochemical exfoliation of graphite represents a simple one-step method that was first reported by Liu and co-workers to produce graphene sheets in ionic liquid/water (electrolyte) mixtures. Here hydroxyl and oxygen radicals produced by anodic oxidation of water start the oxidation of the edge planes of graphite, facilitating intercalation of anions from the ionic liquid. Electrolytes used in this method are surfactant and H_2SO_4–KOH solutions which serve different functions in the process. Though the surfactants prevent re-agglomeration of the graphene and affects electrical/electrochemical properties of graphene, their removal is difficult process. H_2SO_4 used helps in exfoliation of graphite by intercalating and KOH is used to prevent high level of oxidation. In this method, graphitic flakes are obtained with some few layer graphene which are separated by centrifugation [26].

2.8.1.3 SOLVENT-ASSISTED EXFOLIATION

In this method, exfoliation of natural graphite in different solvent is done to produce high concentration of graphene. Different solvents have different processing condition for graphite exfoliation like exfoliation time, using sonication probe instead of sonication bath etc. In new strategy, different types of aqueous surfactant solution are used for exfoliation of natural graphite to avoid expensive and hazardous solvents. In addition, the surfactants can prevent re-aggregation of the graphene due to the repulsive potential barrier between surfactant coated sheets, the importance of which has been studied with regard to graphene dispersion for both ionic and non-ionic surfactants [27].

2.8.1.4 MICROMECHANICAL CLEAVAGE

This type of method is also termed as peel-off or scotch tape method. This method involves the exfoliation of graphite using adhesive tape to cleave the graphene layers apart. Repeated cleavage yields mono-, bi- and few-layer graphene. These can be identified by transferring them on to silicon wafer and using microscopic observation technique e.g. optical microscopy that gives clear contrast difference due to refractive index difference between graphene sheets and silicon wafer. This method is slow and labour intensive but gives high purity graphene, so the material produced is often reserved for study of the fundamental properties of graphene rather than use in commercial applications [28-29].

2.8.1.5 EXFOLIATION OF GRAPHITE OXIDE

This is the chemical method for obtaining graphene from graphite. Graphite oxide is synthesised via oxidation of graphite using concentrated acids and strong oxidants. Graphene is obtained by exfoliation of graphite oxide by sonication or thermally into graphene oxide (GO), followed by reduction of graphene oxide to produce graphene. The resulting material is generally termed reduced graphene oxide (rGO).

2.8.1.6 UNZIPPING OF CARBON NANOTUBES

Synthesis of graphene or few layer graphene from single or multi walled carbon nanotubes can be done by unzipping it with strong oxidizing agents or by physical methods such as laser irradiation and plasma etching. The unzipping results in graphene nano ribbons (i.e. thin, elongated strips of graphene that possess straight edges) that are produced by lengthwise cutting and unravelling of multi-wall carbon nanotubes' (MWCNTs) side walls. Graphene nanoribbons are considered as quasi one dimensional material and have different properties depending on their width and edge type (armchair or zigzag). Carbon nanotube unzipping occurs via C–C bond fission which is often initiated at defect sites, leading to irregular cutting [30-31].

2.8.2 BOTTOM-UP METHODS

2.8.2.1 EPITAXIAL GROWTH ON SILICON CARBIDE

Another method of obtaining graphene is to heat silicon carbide (SiC) to high temperatures (>1,100 °C) under low pressures (~10^{-6} torr) to reduce it to graphene The formation of

graphene on silicon carbide (SiC) proceeds via the preferential sublimation of silicon from the SiC surface and subsequent graphitisation of the excess carbon atoms left behind.

This process produces epitaxial graphene with dimensions dependent upon the size of the SiC substrate (wafer). The face of the SiC used for graphene formation i.e. silicon- or carbon-terminated, highly influences the thickness, mobility and carrier density of the graphene. The two major drawbacks of this method are the high cost of the SiC wafers and the high temperatures (above 1,000 ^{0}C) used, which are not directly compatible with silicon electronics technology [32].

2.8.2.2 CHEMICAL VAPOUR DEPOSITION

In chemical vapour deposition (CVD), graphene is formed by the high temperature pyrolysis of carbon containing gases. This method has been widely used to grow graphene films on transition metal substrates and represents a very active area of graphene research. CVD graphene growth can be categorised as proceeding through either surface catalysed or segregation methods depending on the metal. For surface catalysed reactions, the decomposition of the carbon containing species and graphene formation occur at the metal surface and growth can be described as "self-limiting" to monolayer graphene as the surface is pacified once covered. For segregation, graphene forms via the diffusion of carbon dissolved in the bulk metal to the metal surface, which generally occurs upon cooling due to the reduced solubility of carbon in metals at lower temperatures. The number of graphene layers produced by segregation depends on various factors including the amount of carbon dissolved and the rate of cooling. The optimum conditions for CVD growth vary depending on the metal with different factors (pressure, temperature and carbon exposure) impacting graphene quality and thickness to different extents depending on the system [33].

2.9 OVERVIEW OF GRAPHITE OXIDE

Graphite oxide, formerly called graphitic oxide or graphitic acid, is a compound of carbon, oxygen, and hydrogen in variable ratios, obtained by treating graphite with strong oxidizers. The maximally oxidized bulk product is a yellow solid with C/O ratio between 2.1 to 2.9, that retains the layer structure of graphite but with a much larger and irregular spacing.

Graphite oxide was first prepared by the British chemist B. C. Brodie in 1859, and became very popular in the scientific community during the last half decade, simply because it was believed to be an important precursor to graphene (a single atomic layer of graphite, the

discovery of which won Andre Geim and Konstantin Novoselov the 2010 Nobel Prize in Physics). Graphite oxide is an important functional derivative of grapheme considering the fact that there has been increasing interest in the scientific community in investigating different aspects, particularly the surface modification of graphene. Such functionalization and dispersion of graphene sheets are of crucial importance for their processing and realization of applications [34-35].

2.10 SYNTHESIS OF GRAPHITE OXIDE

Graphite oxide is not a naturally occurring compound. Generally it is prepared by chemical method involving oxidation of suitable graphite source. Different methods and modifications have been developed over the years for fast and hazard free synthesis of graphite oxide.

2.10.1 BRODIE AND STAUDENMAIER METHODS

B.C. Brodie, a British chemist prepared the first batch of GO when he was investigating the chemistry of graphite in 1859. He prepared graphite oxide by adding $KClO_3$ into slurry of graphite in fuming HNO_3, after washing and drying of this slurry a light yellow colour product was obtained. The process was extremely laborious and time consuming involving explosion hazards [35].

The first improvement on Brodie's work happened in 1898 by L. Staudenmaier. He made two changes in Brodie's process first added sulphuric acid to increase the acidity of the mixture second added multiple aliquots of potassium chlorate solution into the reaction mixture over the course of reaction. These changes led to a highly oxidized GO product in a single reaction vessel, thus largely simplified GO synthesis process with the same product composition as Brodie. However, Staudenmaier's method was again both time consuming and hazardous: the addition of potassium chlorate typically lasted over a week, and the chlorine dioxide evolved needed to be removed by an inert gas, while explosion was a constant hazard. Therefore, further modification or development of this oxidation process was still worth investigation [36].

2.10.2 HUMMER'S METHOD AND ITS MODIFICATIONS

Nearly 60 years after Staudenmaier's strategy, chemists Hummers and Offeman in Mellon Institution of Industrial Research developed a different oxidation method for making GO from graphite. A water-free mixture of concentrated sulphuric acid, sodium nitrate and potassium permanganate was prepared and maintained at temperature below 45 °C for

graphite oxidation. After complete oxidation of graphite, final product with higher degree of oxidation than Staudenmaier's product was obtained. Modifications in Hummers method have been done by other researchers by increasing the amount of potassium permanganate or oxidising agent [37].

2.11 STRUCTURE AND PROPERTIES OF GRAPHITE OXIDE

The structure and properties of graphite oxide depend on particular synthesis method and degree of oxidation. Since graphite oxide is prepared from oxidation of graphite, compared to pristine graphite, graphite oxide is heavily oxygenated bearing hydroxyl and epoxy groups on sp^3 hybridized carbon on the basal plane, in addition to small amount of lactol, ester, acid, ketone and carbonyl groups located at the sheet edges on sp^2 hybridized carbon. Hence, GO is highly hydrophilic and readily exfoliated in water, yielding stable dispersion consisting mostly of single layered sheets (graphene oxide). It is important to note that although graphite oxide and graphene oxide have similar chemical properties i.e. both have same surface functional groups on the surface, their structures are different. Graphene oxide is a monolayer material produced by the exfoliation of graphite oxide. Sufficiently dilute colloidal suspension of graphene oxide prepared by sonication remains clear, homogeneous and stable. The pristine graphite sheet is atomically flat but graphene oxide sheets are thicker due to the displacement of sp^3 hybridized carbon atoms slightly above and below the original graphene plane and presence of covalently bound oxygen atoms [38, 39].

.

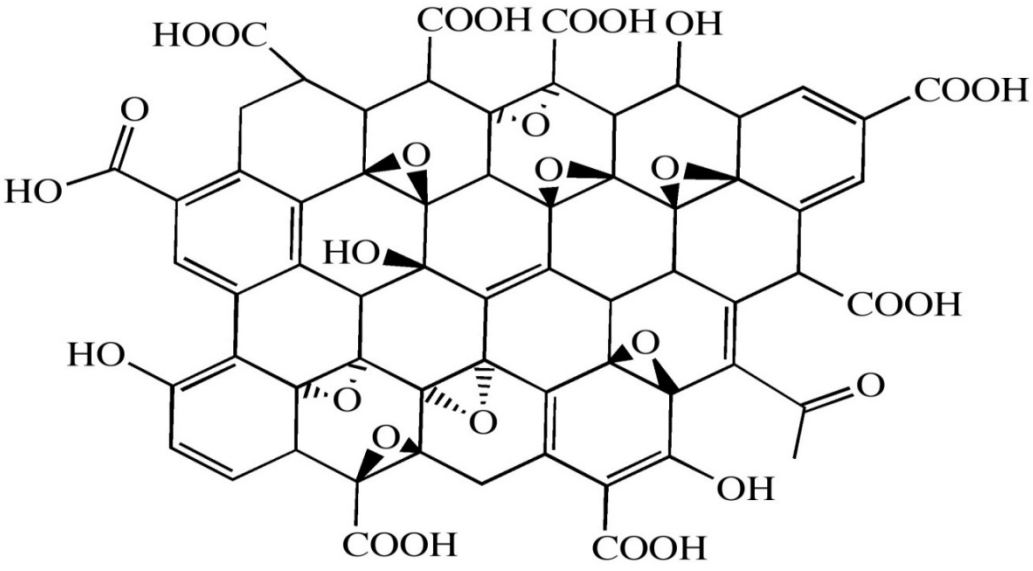

Fig 7: Chemical structure of graphite oxide.

2.12 REDUCTION OF GRAPHITE OXIDE

The presence of oxygenated functional groups on the surface of graphite oxide provides reactive sites for a variety of surface-modification reactions to develop functionalized graphene oxide- and graphene-based materials. On the other hand, due to the disruption of the conjugated electronic structure by these functional groups, graphene oxide becomes electrically insulating and contained irreversible defects and disorders but reduction of graphene oxide could partially restore its conductivity at values orders of magnitude below that of pristine graphene. Different strategies have been used to reduce graphene oxide like thermal or chemical reduction.

2.12.1 THERMAL REDUCTION

GO can be reduced solely by heat treatment and the process is named thermal annealing reduction. In the initial stages of graphene research, rapid heating (>2000 ^{0}C/min) were usually employed to exfoliate graphite oxide to achieve graphene. The mechanism of exfoliation is mainly the sudden expansion of CO or CO_2 gases evolved into the spaces between graphene sheets during rapid heating of the graphite oxide. The rapid temperature increase makes the oxygen containing functional groups attached on carbon plane to decompose into gases that create huge pressure between the stacked layers. The exfoliated sheets can be directly named graphene (or chemically derived graphene) rather than GO, which means that the rapid heating process not only exfoliates graphite oxide but also reduces the functionalized graphene sheets by decomposing oxygen-containing groups at elevated temperature. This dual-effect makes thermal expansion of graphite oxide a good strategy to produce bulk quantity graphene. However, this procedure is found only to produce small size and wrinkled graphene sheets. This is mainly because the decomposition of oxygen-containing groups also removes carbon atoms from the carbon plane, which splits the graphene sheets into small pieces and results in the distortion of the carbon plane [40]

Thermal annealing is usually carried out by thermal irradiation. As an alternative, some unconventional heating resources have been tried to realize thermal reduction including microwave irradiation (MWI) and photo-irradiation. The main advantage of MWI over conventional heating methods is heating substances uniformly and rapidly. By treating graphite oxide powders in a commercial microwave oven, rGO can be readily obtained within 1 min in ambient conditions [41].

2.12.2 CHEMICAL REDUCTION

Chemical reduction of GO is based on the reactivity between reducing agent and GO functional groups. Chemical reduction of graphene oxide with hydrazine was first done by Stankovich et al. The reduction by hydrazine and its derivatives, e.g. hydrazine hydrate and dimethyl hydrazine, are achieved by adding the liquid reagents to a GO aqueous dispersion. This aqueous dispersion reduction process results in agglomerated graphene-based nanosheets due to the increase of hydrophobicity. The increase in hydrophobicity is due to the removal of oxygenated functional groups from the graphite oxide surface [42].

Metal hydrides, e.g. sodium hydride, sodium borohydride ($NaBH_4$) and lithium aluminium hydride are strong reducing reagents used in organic chemistry. These reagents are used for the reduction of functional groups like carboxylic acid, ester, carbonyl, hydroxyl etc. But the main drawback of above these reagents is their very strong reactivity with water. On the other hand, water is main solvent for the exfoliation and dispersion of GO. Hence these reducing agents are generally not used for reduction of GO exfoliated in water. $NaBH_4$ has been found to be more effective reductant for GO than hydrazine. . Further, $NaBH_4$ is most effective at reducing C=O species but has low to moderate efficiency in the reduction of epoxy groups and carboxylic groups hence remains unreduced [43].

Ascorbic acid is a newly reported reducing reagent for GO, which is considered to be an ideal substitute for hydrazine. In addition, ascorbic acid has number of advantages e.g. its non-toxicity in contrast to hydrazine and a higher chemical stability with water than $NaBH_4$. Besides, the reduction in colloid state does not result in the aggregation of rGO sheets as produced by hydrazine, which is beneficial for further applications. Graphene obtained from reduction of GO with ascorbic acid has comparable conductivity with hydrazine reduced graphene (figure 8) [44-45].

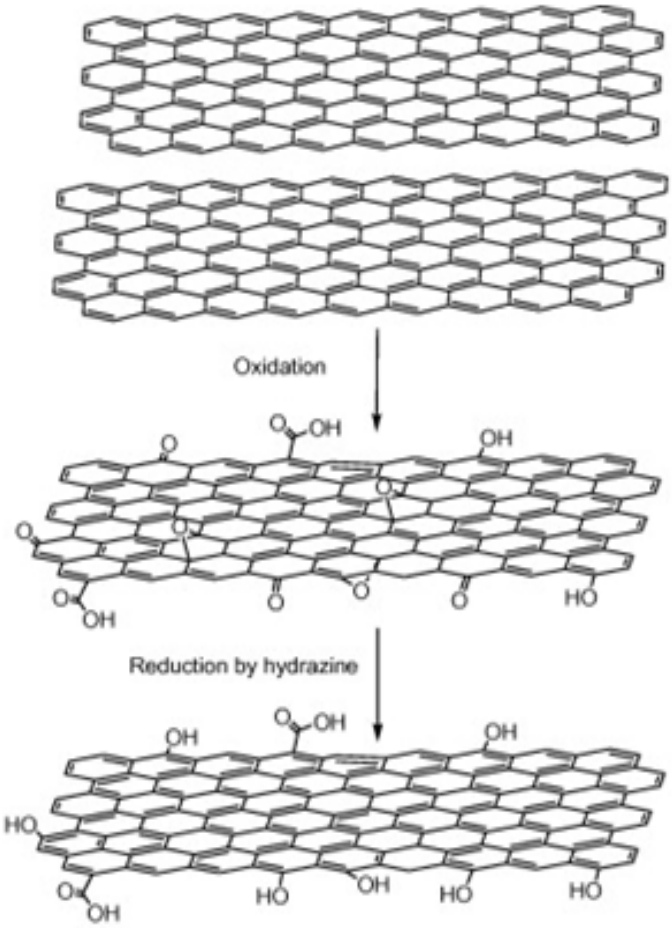

Fig 8: Graphene synthesis by Chemical Oxidation-Reduction.

CHAPTER 3
MATERIALS AND METHOD

3.1 RAW MATERIAL

- Graphite powder (CDH, India),
- Sodium nitrate $NaNO_3$ (Fischer scientific),
- Potassium permanganate $KMnO_4$ (Fischer scientific)
- Sulphuric Acid H_2SO_4, 98% (Merc chemicals)
- Hydrogen Peroxide H_2O_2 ,30% (Speck pure chemicals)
- Hydrazene Hydrate $NH_2NH_2.H_2O$ (Thomas Baker)
- Cotton-polyester fabric

- Number of threads in warp direction (in 1 cm) ~30
- Number of threads in warp direction (in 1 cm) ~ 25

3.2 SYNTHESIS OF GO

Natural graphite powder was oxidized to GO using modified Hummers method. In a typical synthesis, 5 g of graphite and 5 g of sodium nitrate ($NaNO_3$) were added into 200 mL concentrate H_2SO_4 in an ice bath followed by the gradual addition of 30 g of $KMnO_4$ and during the addition the temperature was kept below 30 °C since reaction is exothermic. Afterward, the reaction mixture was placed under stirring at room temperature for 18 h, forming a thick paste. Subsequently, the paste was gradually poured into 400 mL deionised water. After 20 min. another 1 L of deionised water was added to the mixture followed by the drop wise addition of 30 mL of 30 % H_2O_2 solution to reduce the excess $KMnO_4$. The solution turns light brown after the addition of H_2O_2, it was decanted and centrifuged followed by washing with deionised water till the pH was 7 and dried at room temperature under vacuum for 24 h to obtain GO solid.

3.3 PREPARATION OF GO COATED COTTON-POLYESTER FABRIC

Initially cotton-polyester fabric was washed to remove any surface finish present on the surface. After that aqueous dispersion of GO with the concentration of 1mg/ml, 2mg/ml, 4mg/ml were exfoliated using ultrasonic bath for 40 minute. The cotton-polyester fabrics was immersed in exfoliated GO solution (1mg/ml) for 15 minute, removed and dried. This process was repeated several times to increase GO loading on the cotton fabric and the fabric was coded as 1FGO. Similarly, GO coated fabrics treated with 2mg/ml and 4 mg/ml GO solutions were also formed and named as 2FGO and 3FGO respectively. The loading level of GO was calculated from the weight difference between the fabrics before and after GO coating.

3.4 PREPARATION OF GRAPHENE COATED FABRIC

GO coated fabric was exposed to hydrazine hydrate solution for 8 h to bring about the reduction. Subsequently, the reduced GO coated fabric was dried for an hour at 60 ^{0}C. The amount of the graphene deposited on the fabric was determined by reweighing fabric on an electronic balance (Sartorius with 10^{-4} precision). In analogy to their GO coated counterparts, the obtained reduced GO coated fabrics were coded as 1RVFGO, 2RVFGO and 3RVFGO.

(a)

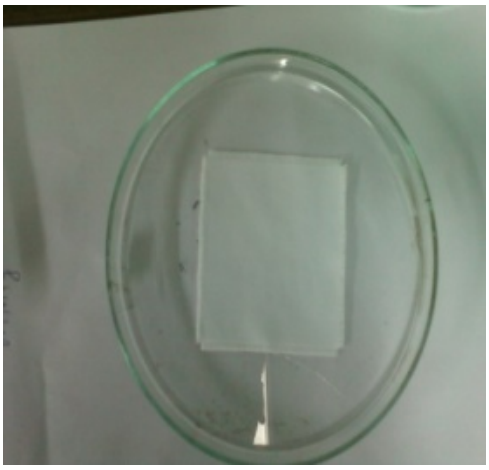

(b)

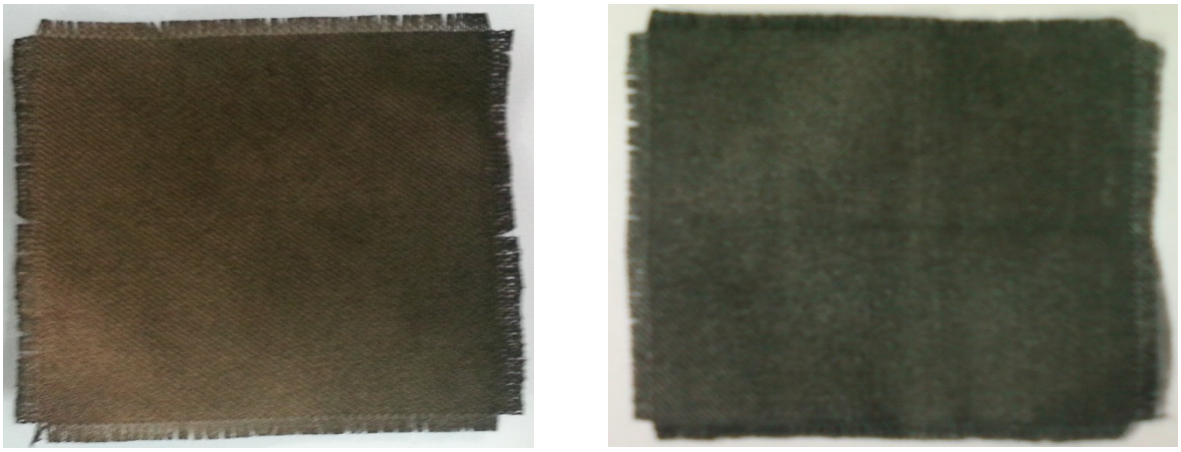

(c) **(d)**

Fig 9: (a) GO, (b) Pure fabric, (c) GO coated fabric, (d) Graphene coated fabric

3.5 CHARACTERISATION TECHNIQUES

3.5.1 HIGH RESOLUTION TRANSMISSION ELECTRON MICROSCOPY (HRTEM)

High-resolution transmission electron microscopy (HRTEM) is an imaging mode of the transmission electron microscope (TEM) that allows for direct imaging of the atomic structure of the sample. Transmission electron microscopy (TEM) is a microscopy technique whereby electrons beam is transmitted through an ultra-thin specimen, interacting with the specimen as it passes through. An image is formed from the interaction of the electrons transmitted through the specimen; the image is magnified, and focused onto an imaging device, such as fluorescent screen, on photographic film layer or detected by a sensor like CCD camera. TEM provides very high resolution (~ 0.5nm) image and diffraction pattern of the specimen. The highly energetic electron beam (300 KeV) interacts with target material (< 200 nm) to provide materials characterization using backscattered, secondary electron and EDS imaging. HRTEM is a powerful tool to study properties of materials on the atomic scale, such as semiconductors, metals, nanoparticles and sp^2-bonded carbon e.g. graphene, carbon nanotubes.

Fig 10: HRTEM instrument

Transmission electron microscopy characterization of graphene oxide was performed using a TEM microscope TM model Technai G2F30 S Twin, The Netherlands. A droplet of GO dispersion was cast on to a TEM copper grid and solvent was evaporated at room temperature.

3.5.2 SCANNING ELECTRON MICROSCOPY (SEM)

Surface morphology of Nanostructure has been carried out by SEM. In this technique, high energy (few hundred eV to 100 KeV) electrons (emitted from a tungsten or lanthanum hexaboride (LaB_6) as cathode) are focused (focal spot sized 1 nm to 5 nm) on a specimen using electromagnetic condenser lenses to see three dimensional information of surface of a specimen or object. Because of small wavelength of electron waves, resolution of image is quite high. The beam passes through pairs of scanning coils in the objective lens, which deflect the beam horizontally and vertically so that it scans over a rectangular area of the sample surface. When the primary electron beam interacts with the sample, the electrons lose energy by repeated scattering and absorption within the interaction volume, which extends from less than 100 nm to around few micrometers into the surface which depends on the beam accelerating voltage, the atomic number of the specimen and the specimen's density. The electrons are detected by a scintillator-photomultiplier device and the resulting signal is rendered into a two dimensional intensity distribution that can be viewed and saved as a digital image. The brightness of the signal depends on the secondary electrons reaching the detector and this number depends on the surface (flat, steep surface and edges).

Fig 11: SEM Instrument

Surface morphology of the washed fabric, 1FGO, 2FGO, 3FGO, 1RVFGO, 2RVFGO, 3RVFGO was examined by EDS LEO 440 scanning electron microscope after sputter coating with a very thin layer of Au.

3.5.3 RAMAN SPECTROSCOPY

Raman spectroscopy provides key information about the structure of molecules. The position and intensity of features in the spectrum reflect the molecular structure and is used to determine the chemical identity of the sample. Spectra also show changes depending on the crystalline form. Raman is a light scattering technique, which measures the shift in frequency from that of the excitation laser. For the collection of Raman spectrum sample is placed into path of the excitation beam and spectrum from scattered beam is collected.

Renishaw Raman spectrometer was used for recording Raman spectrum of samples. These spectra were recorded using diode laser at 514 nm excitation with Raman shift between 500 cm^{-1} - 3000 cm^{-1}

3.5.4 FOURIER TRANSFER INFRARED SPECTROSCOPY (FTIR)

Fourier Transform Infrared Spectroscopy (FTIR) is a powerful tool for identifying structure information, types of chemical bonds in a molecule by producing an infrared absorption spectrum that is like a molecular "fingerprint. It is a technique which is used to obtain an infrared spectrum of absorption, emission, or Raman scattering of a solid, liquid or gas.

In Fourier Transform Infrared Spectroscopy sample is shined by a beam containing many frequencies of light at once rather than shining single wavelength as in normal absorption spectroscopy, and measures how much of that beam is absorbed by the sample. Next, the

beam is modified to contain a different combination of frequencies, giving a second data point. This process is repeated many times. Afterwards, a computer takes all these data and works backwards to infer what the absorption is at each wavelength. This processing of data is done on algorithm called Fourier Transform.

Samples for FTIR characterization are prepared in a number of ways. For liquid samples, the easiest is to place one drop of sample between two plates of sodium chloride (salt). Salt is transparent to infrared light. The drop forms a thin film between the plates. Solid samples can be milled with potassium bromide (KBr) to form a very fine powder. This powder is then compressed into a thin pellet which can be analyzed. KBr is also transparent in the IR. Alternatively, solid samples can be dissolved in a solvent such as methylene chloride, and the solution placed onto a single salt plate. The solvent is then evaporated off; leaving a thin film of the original material on the plate. This is called a cast film, and is frequently used for polymer identification. Solutions can also be analyzed in a liquid cell.

The FTIR spectra of powder samples of graphite and GO were recorded on Thermo scientific Nicolet 380 spectrometer in the wave number range 400-4000 cm^{-1} at a resolution of 4 cm^{-1} and averaged over 32 scans.

3.5.5 POWDER X-RAY DIFFRACTION (XRD)

Powder X-ray diffraction analysis has been used to identify the average crystallite size, unit cell structure, lattice parameter, miller indices, phases present in the material, crystalline/amorphous property of the sample. The basic principle of X-ray diffraction, as postulated by Von Lave, says that if X-rays are waves and the distances between atoms in solids are comparable to wavelength of X-ray then they should be diffracted by atoms in the solids.

The diffraction of X-rays in crystals is determined by the Bragg diffraction condition which is as follows:

$$2d.\sin\theta = n\lambda$$

Where n = 1, 2, 3, …

The diffraction pattern from different type of samples such as single crystals, amorphous samples, nanocrystalline samples, liquids etc. is entirely different.

Figure 11 shows bragg diffraction. Two beams with identical wavelength and phase approach a crystalline solid and are scattered off two different atoms within it. The lower beam

traverses an extra length of $2d\sin\theta$. Constructive interference occurs when this length is equal to an integer multiple of the wavelength of the radiation i.e.

$$2d.\sin\theta = n\lambda$$

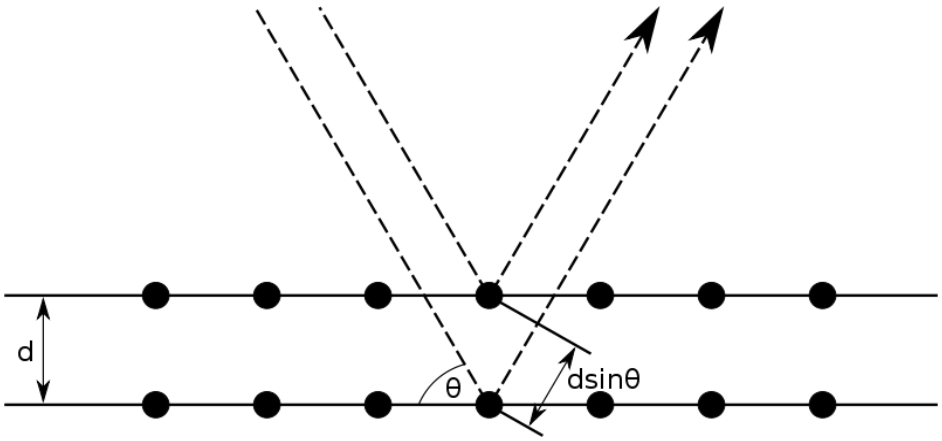

Fig 12: Bragg diffraction pattern

The XRD patterns were recorded using Bruker D8 Advance X-ray diffractometer in the diffraction (2θ) range of 5-80^{o}, at a scan rate of 0.2/sec, slit width of 0.1 mm using CuKα line (λ= 1.540598Å) as radiation source.

3.5.6 THERMO GRAVIMETRIC ANALYSIS (TGA)

Thermo gravimetric analysis or thermal gravimetric analysis (TGA) is a method of thermal analysis in which changes in physical and chemical properties of materials are measured as a function of increasing temperature with constant heating rate, or as a function of time with constant temperature and/or constant mass loss.

TGA can provide information about physical phenomena, such as second-order phase transitions, including vaporization, sublimation, absorption, adsorption, and desorption. Likewise, TGA can provide information about chemical phenomena including chemisorptions, desolvation (especially dehydration), decomposition, and solid-gas reactions (e.g., oxidation or reduction) TGA is commonly used to determine selected characteristics of materials that exhibit either mass loss or gain due to decomposition, oxidation, or loss of volatiles such as moisture. Common applications of TGA are-

(1) Materials characterization through analysis of characteristic decomposition patterns,

(2) Studies of degradation mechanisms and reaction kinetics,

(3) Determination of organic content in a sample, and

(4) Determination of inorganic (e.g. ash) content in a sample, which may be useful for corroborating predicted material structures or simply used as a chemical analysis.

Thermo gravimetric analysis (TGA) of graphite, graphene oxide, washed fabric (WF), 1 FGO, 3FGO, 1RVFGO and 3RVFGO were carried out under N_2 flow using TA Instrument Perkin Elmer Pyris 6 TGA and their masses were recorded as a function of temperature. The samples were heated from room temperature to 800 °C at 20 °C/min, 5±1 mg sample were used in each experiment.

3.5.7 CONTACT ANGLE MEASUREMENT

The phenomenon of wetting or non-wetting of a solid by a liquid is studied by contact angle measurement. The drop of liquid forming an angle may be considered as resting in equilibrium by balancing the three forces involved. Namely, the interfacial tensions between solid and liquid SL, that between solid and vapour SV and that between liquid and vapour LV. The angle within the liquid phase is known as the contact angle or wetting angle. It is the angle included between the tangent plane to the surface of the liquid and the tangent plane to the surface of the solid, at any point along their line of contact. The surface tension of the solid favours spreading of the liquid, but this is opposed by the solid-liquid interfacial tension and the vector of the surface tension of the liquid in the plane of the solid surface. If the water contact angle is less than 90^0 surfaces is termed as hydrophilic, if water contact angle is greater than 90^0 surfaces is termed as hydrophobic. Contact angle are measured by dynamic Sessile or Wilhelmy method. In sessile drop method contact angle is measured by goniometer using an optical subsystem to capture the profile of a pure liquid on a solid substrate.

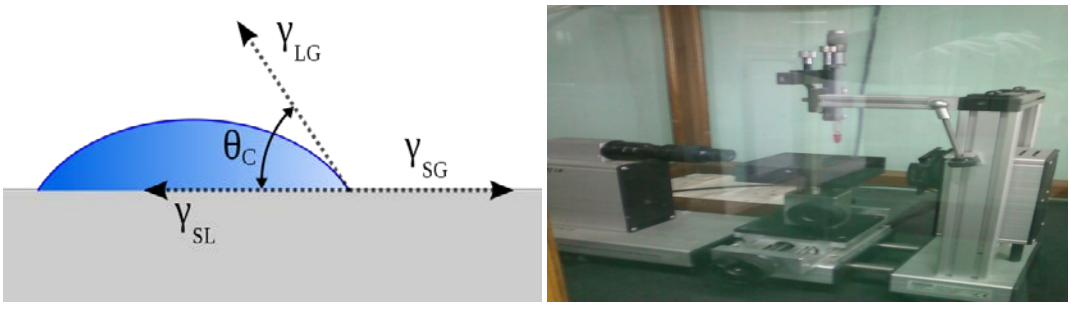

Fig 13: Contact angle & contact angle measurement instrument

Water contact angles were recorded on a drop shape analysis system; model DSA10MK2 from Krüss GmbH, Germany using sessile drop method.

3.5.8 MECHANICAL TESTING

Tensile testing of fabric samples were performed on UTM machine (Instron) on rectangular sample strips of fabric size (50x10x31) mm ±4 mm. Strain rate for tensile measurement was taken 12mm/minute.

Fig 14: UTM machine (Instron)

3.5.9 RESISTANCE/CONDUCTIVITY MEASUREMENT

DC voltage, DC current, and resistance are measured most often with digital multimeters (DMMs). Generally, these instruments are adequate for measurements at signal levels greater than 1μV or 1μA, or less than 1GΩ However, they don't approach the theoretical limits of sensitivity. For low level signals, more sensitive instruments such as electrometers, picoammeters, and nanovoltmeters must be used.

An electrometer is a highly refined DC multimeter. As such, it can be used for many measurements performed by a conventional DC multimeter. Additionally, an electrometer's special input characteristics and high sensitivity allow it to make voltage, current, resistance, and charge measurements far beyond the capabilities of a conventional DMM. An electrometer must be used when any of the following conditions exist: The task requires an extended measurement range unavailable with conventional instruments, such as for detecting or measuring:

• Currents less than 10 nA (10^{-8}A).

• Resistances greater than 1GΩ (10^{9}Ω).

Fig 15: Programmable electrometer

Rectangular sample (3cm X 2cm) was cut from GO coated fabric and graphene coated fabric. Resistance of these fabric samples were taken at 2cm distance using two probe method on Keithley 417 programmable electrometer.

3.5.10 EMI SHIELDING EFFECTIVENESS MEASUREMENT

Electromagnetic interference shielding (EMI) is an undesired electromagnetic (EM) induction triggered by extensive use of alternating current/Voltage which tries to produce corresponding induced signals (Voltage and current) in the nearby electronic circuitry, thereby trying to spoil its performance. The mutual interference among electronic gadgets, business machines, process equipments, measuring instruments and appliances lead to disturbance or complete breakdown of normal performance of appliances.

The shielding efficiency is generally measured in terms of reduction in magnitude of incident power/field upon transition across the shield. Mathematically shielding effectiveness (SE_T) can be expressed in logarithmic scale as per expressions

$$SE_T(dB) = SE_R + SE_A + S_{EM} = 10\log_{10}\left(\frac{P_T}{P_I}\right) = 20\log_{10}\left(\frac{E_T}{E_I}\right) = 20\log_{10}\left(\frac{H_T}{H_I}\right)$$

Where P_I (E_I or H_I) and P_T (E_T or H_T) are the power (electric or magnetic field intensity) of incident and transmitted EM waves respectively. As shown in Fig. 7, three different mechanisms namely reflection (R), absorption (A) and multiple internal reflections (MIRs) contribute towards overall attenuation with SE_R, SE_A and SE_M as corresponding shielding effectiveness components due to reflection, absorption and multiple reflections respectively.

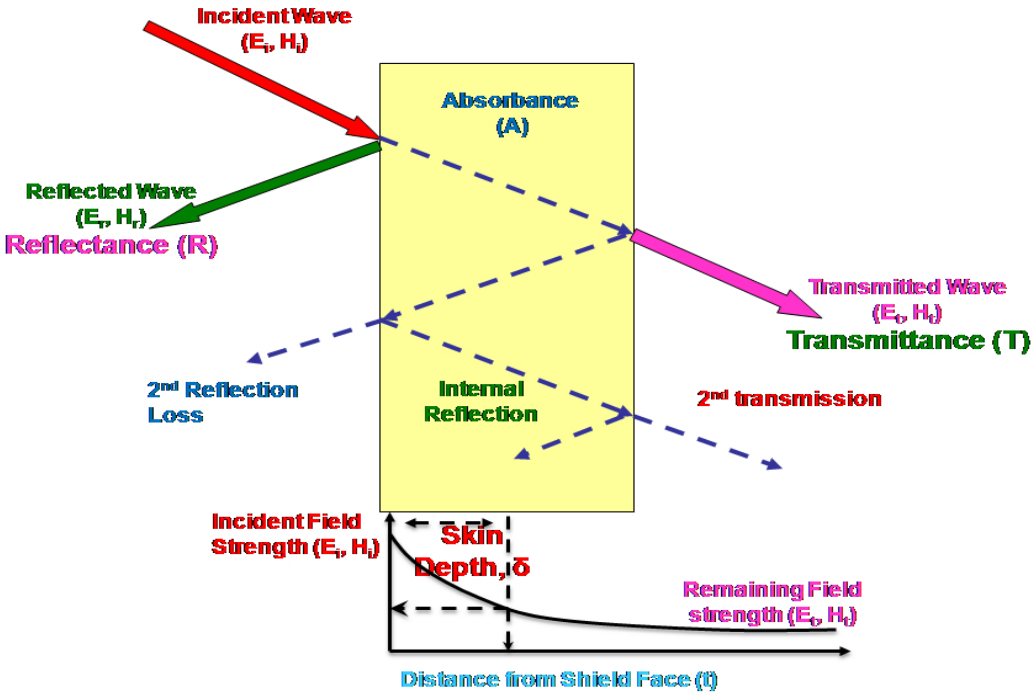

Fig 16: Mechanism of EMI shielding

Shielding effectiveness of graphene coated fabric was measured by free space technique at 101 GHz frequency using microwave measurement setup (Fig. 17) comprising of Aplab DC power supply, 101 GHz microwave frequency generator (source), circular horn type antenna (source), rectangular horn type antenna (receiver) and microwave power meter (detector).

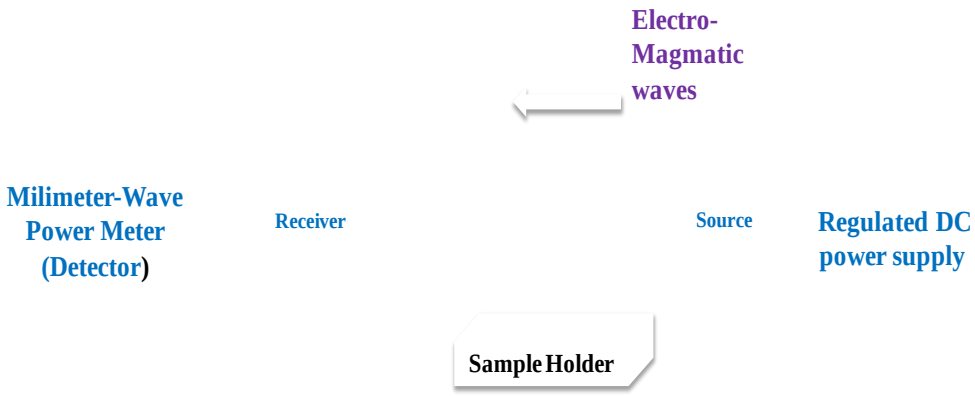

Fig 17: Working of EMI shielding instrument

CHAPTER 4

RESULTS AND DISCUSSION

A: GRAPHITE OXIDE

4.1 THERMO GRAVIMETRIC ANALYSIS

Figure18: shows TG traces of graphite and GO. It can be seen that graphite is quite stable whereas GO show mass loss even below 100 °C which may be due to the pyrolysis of labile oxygen functional groups such as –COOH, -OH etc.

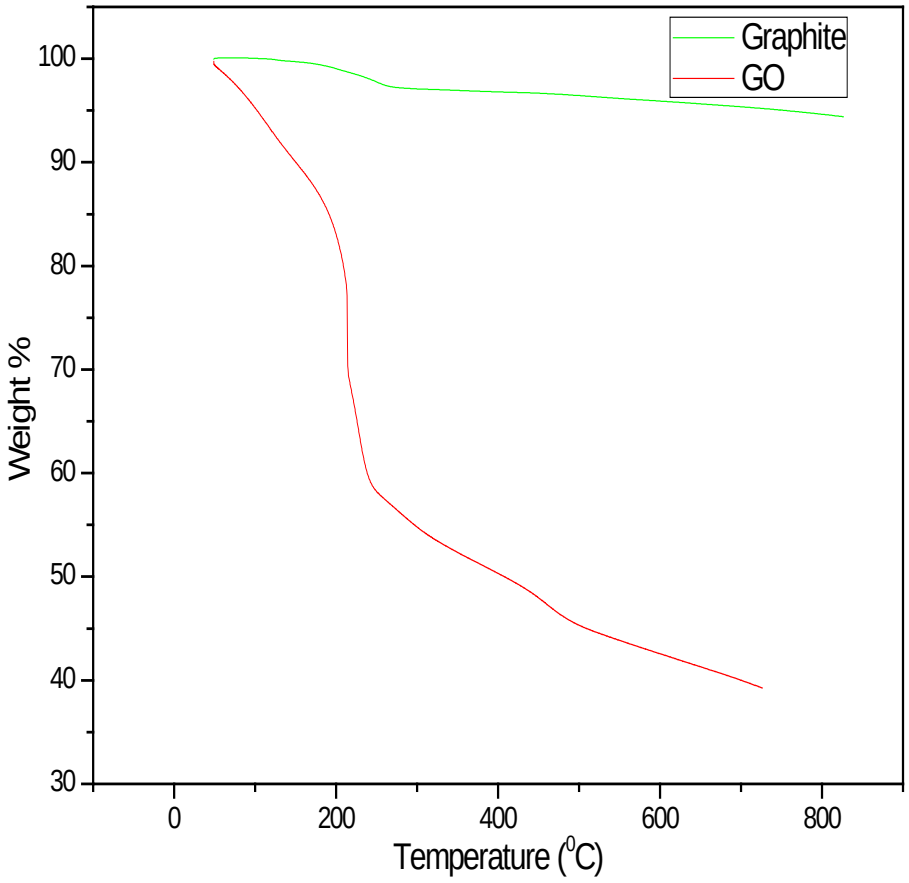

Fig 18: TGA analysis of Graphite and GO

4.2 HIGH RESOLUTION TRANSMISSION ELECTRON MICROSCOPY

Figure 19 shows TEM images of a typical GO nanosheet deposited on a standard TEM grid. The sheet was several micrometers in dimension and display wrinkled rough surface which is characteristic of few layer graphene.

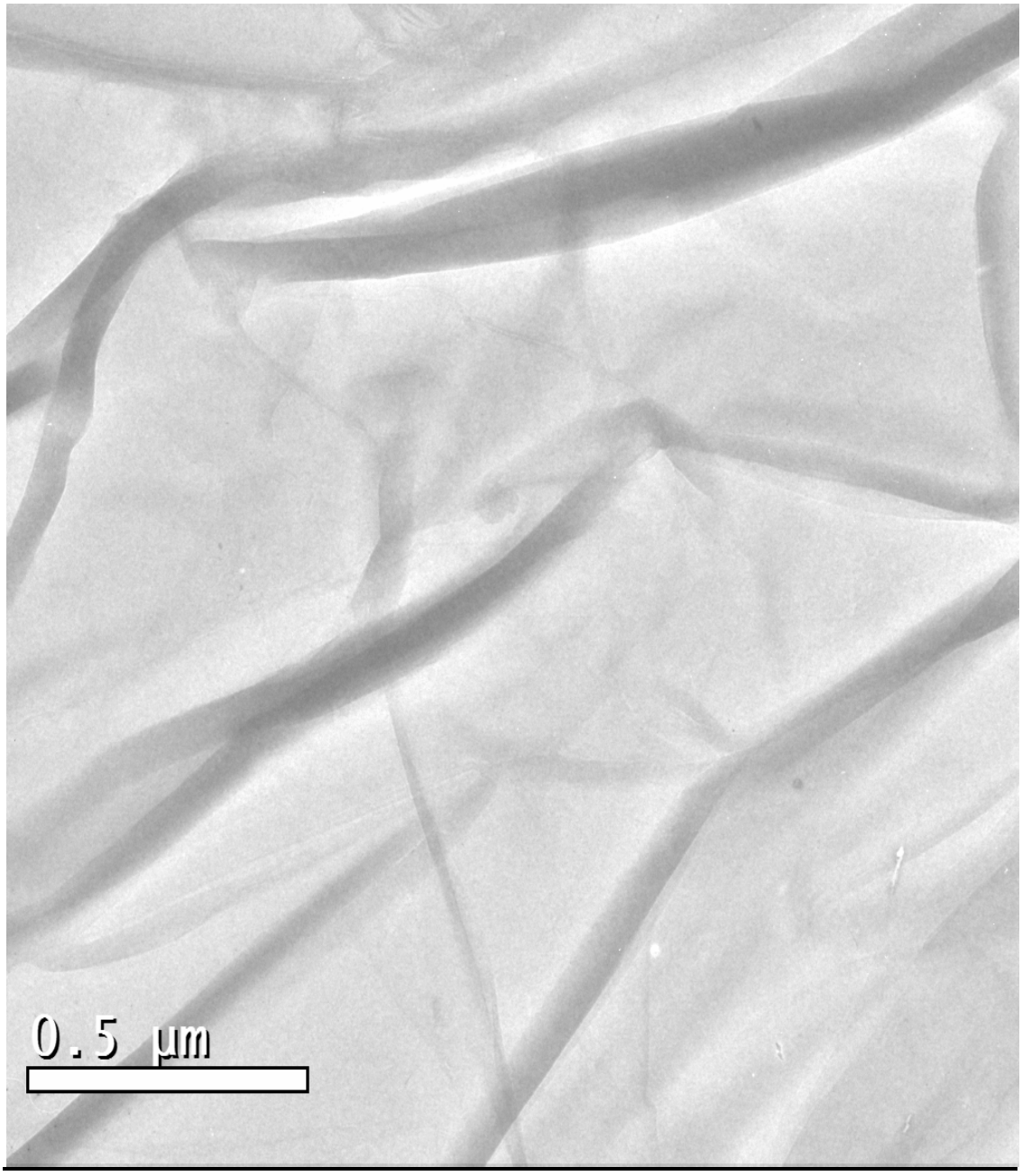

Fig 19: HRTEM image of GO

4.3 RAMAN SPECTROSCOPY

The figure: 20, shows Raman spectra of graphite and graphite oxide. In graphite sample, a single peak at 1582 cm^{-1} is observed that can be attributed to G band associated with the planar configuration of the sp^2 hybridized atoms. In contrast, GO sample gives two peaks corresponding to G-band (at 1582 cm^{-1}) and D band (at 1352cm^{-1}). The D-band is related to the sp^3 hybridization of carbon atom. The presence of D band in GO reflects the disruption of sp^2 hybridization in graphite due to the incorporation of oxygen functionalities (i.e. –OH, –COOH and epoxide groups) and confirms the formation of GO via oxidation of graphite [47].

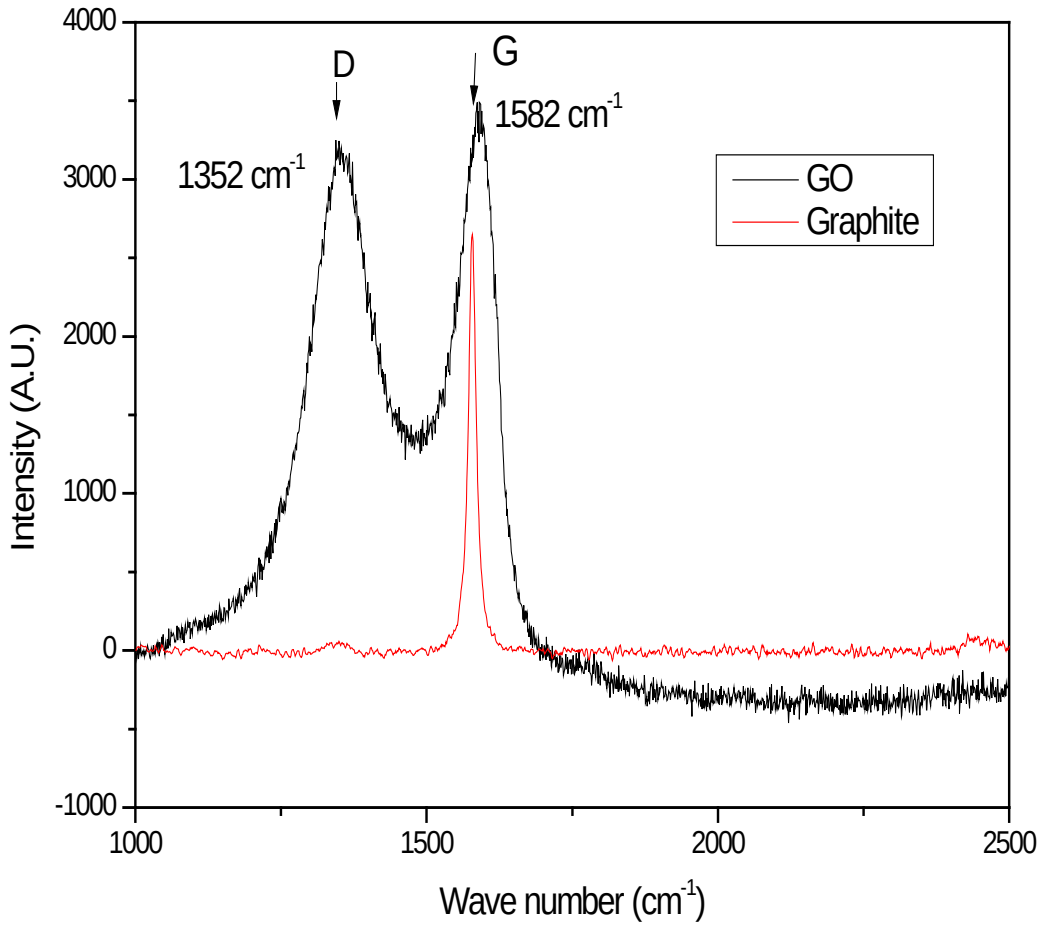

Fig 20: Raman spectra of Graphite and GO

4.4 FTIR SPECTROSCOPY

Figure 21 shows FTIR spectra of graphite and graphite oxide. While no significant peak was found in graphite, the existence of different type of oxygen functionalities in graphite oxide was confirmed by presence of peaks at 3388 cm^{-1} (O-H stretching vibrations), 1727 cm^{-1} (stretching vibrations from C=O), 1617 cm^{-1} (skeletal vibrations from unoxidized graphitic domains), 1225 cm^{-1} (C-OH stretching vibrations) and 1048 cm^{-1} (C-O stretching vibrations) [46].

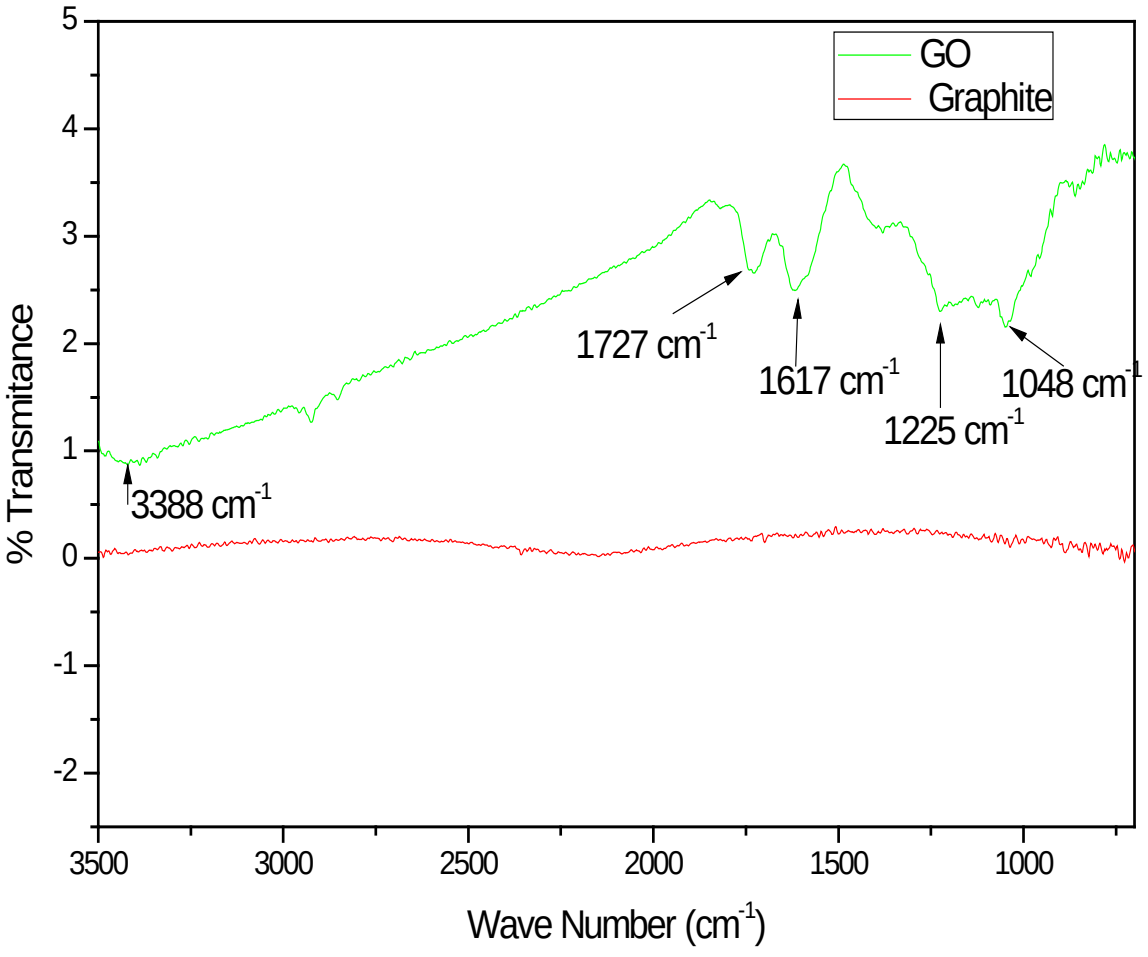

Fig 21: FTIR spectra of graphite and GO

4.5 POWDER X-RAY DIFFRACTION ANALYSIS

Fig-22 shows the XRD pattern of the graphite, and GO. Graphite shows a strong sharp peak at 2θ =26.5^{o}due to the (002) while graphite oxide shows a less intense peak at 2θ = 10.1^{o} compared to graphite. Lowering in the 2θ value of GO is due to the insertion of oxygenated functional groups like –OH, -COOH, epoxy on the plane of graphite surface after oxidation. This was also complemented by the increase in d-spacing from 3.4 Å for pure graphite to 8.9Å for graphite oxide. The above results confirm the successful formation of GO sheets via chemical oxidation of graphite [47].

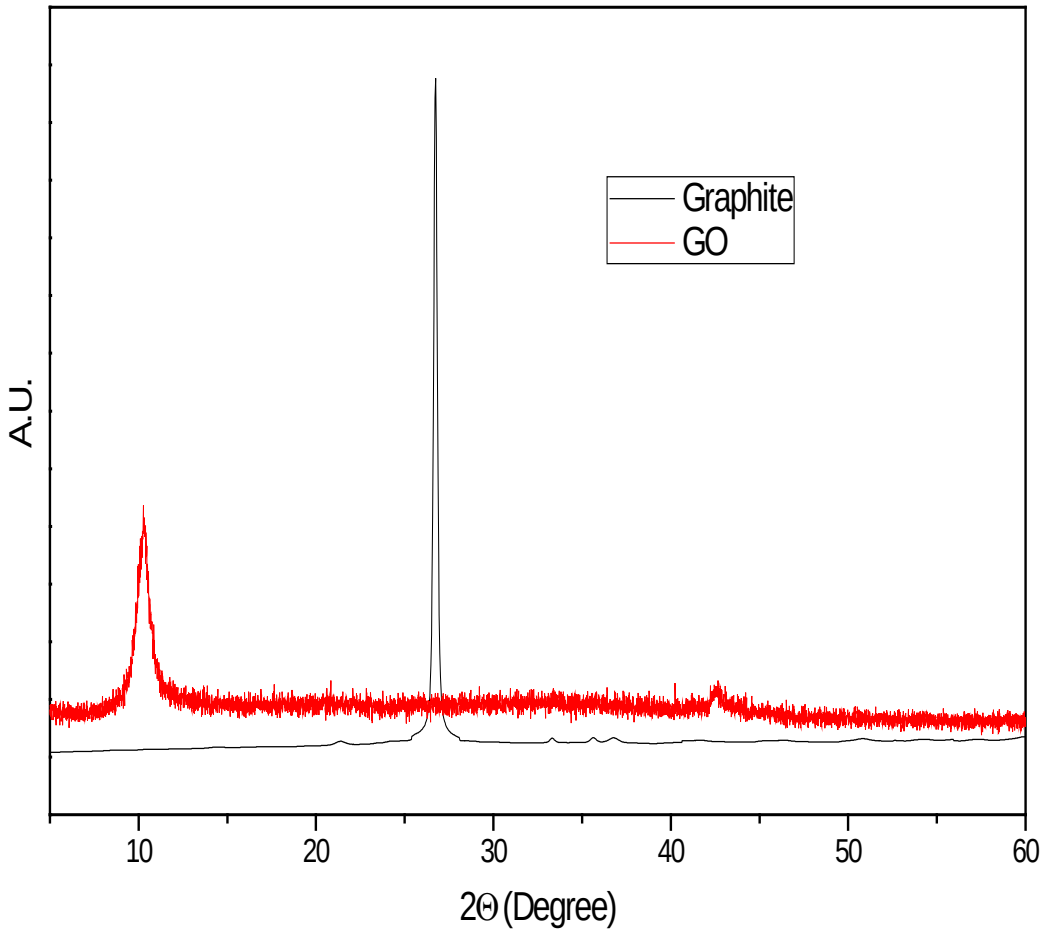

Fig 22: XRD pattern of Graphite and GO

B: FABRIC SAMPLES

4.6 LOADING OF GRAPHENE ON FABRIC SURFACE

Figure 23 and table 2, shows graphene loading on fabric samples.

Table 2: %Loading of graphene on fabric surface

Sample	% Graphene Loading
1RVFGO	2.18
2RVFGO	2.63
3RVFGO	3.75

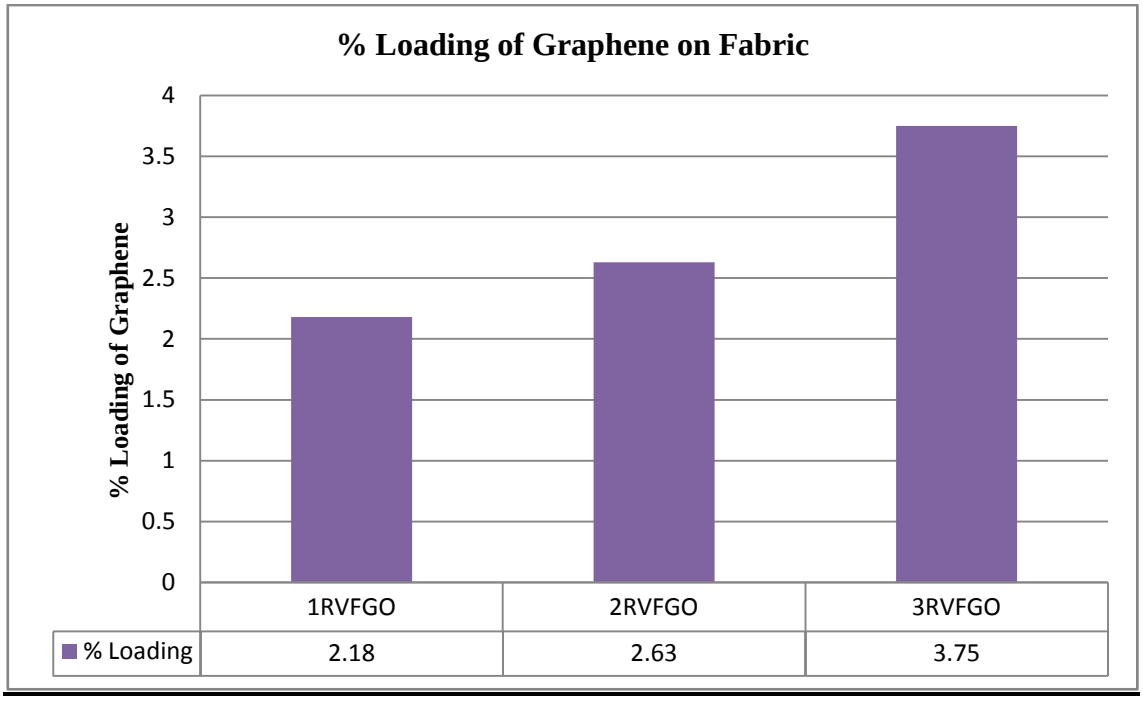

Fig 23: % Loading of graphene on fabric surface.

4.7 SCANNING ELECTRON MICROSCOPY

The SEM image of pure cotton–polyester fabric (Fig. 24a) shows smooth and flat surface. In comparison, the SEM images of GO coated fabric 1FGO, 3FGO (Fig 24 b, c) show the smooth and uniform coating of GO layers over individual fibres. The coating is stabilized by the Van der Waals forces as well as interactions between oxygen functionalities over GO surface and cellulosic groups present on the fibers. As the GO loading level increases, coatings become non-uniform with presence of looses sheets and agglomerates over fibers as well as between inter-fiber regions (weaves). The same trend can be seen in reduced GO coated fabrics 1RVFGO, 3RVFGO (Fig 24 d, e) with increased brightness compared to GO coated fabrics due to the increased conductivity of fabrics. This reveals the presence of graphene sheets over fibers/fabrics after the reduction of coated GO phase.

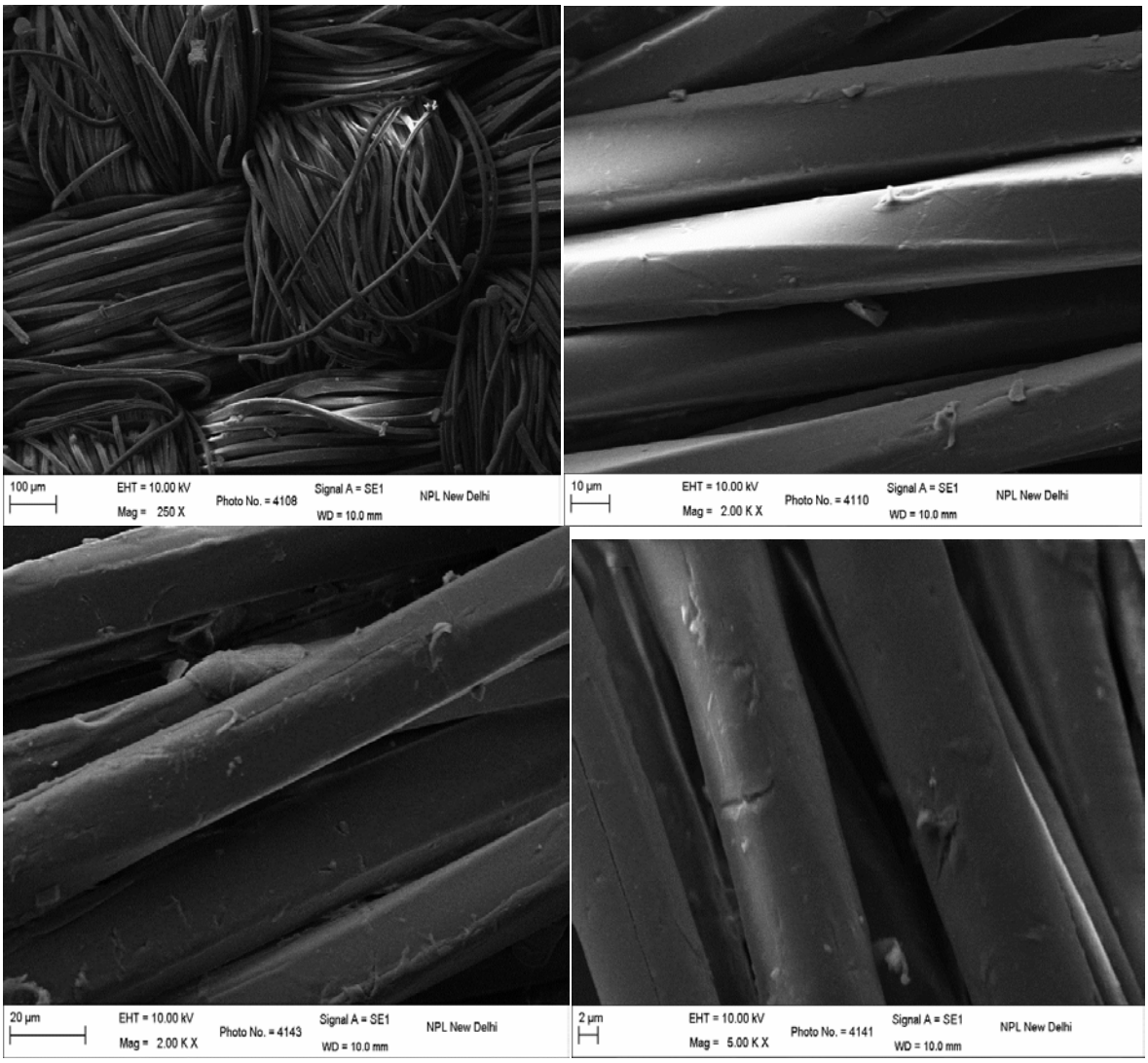

(a)

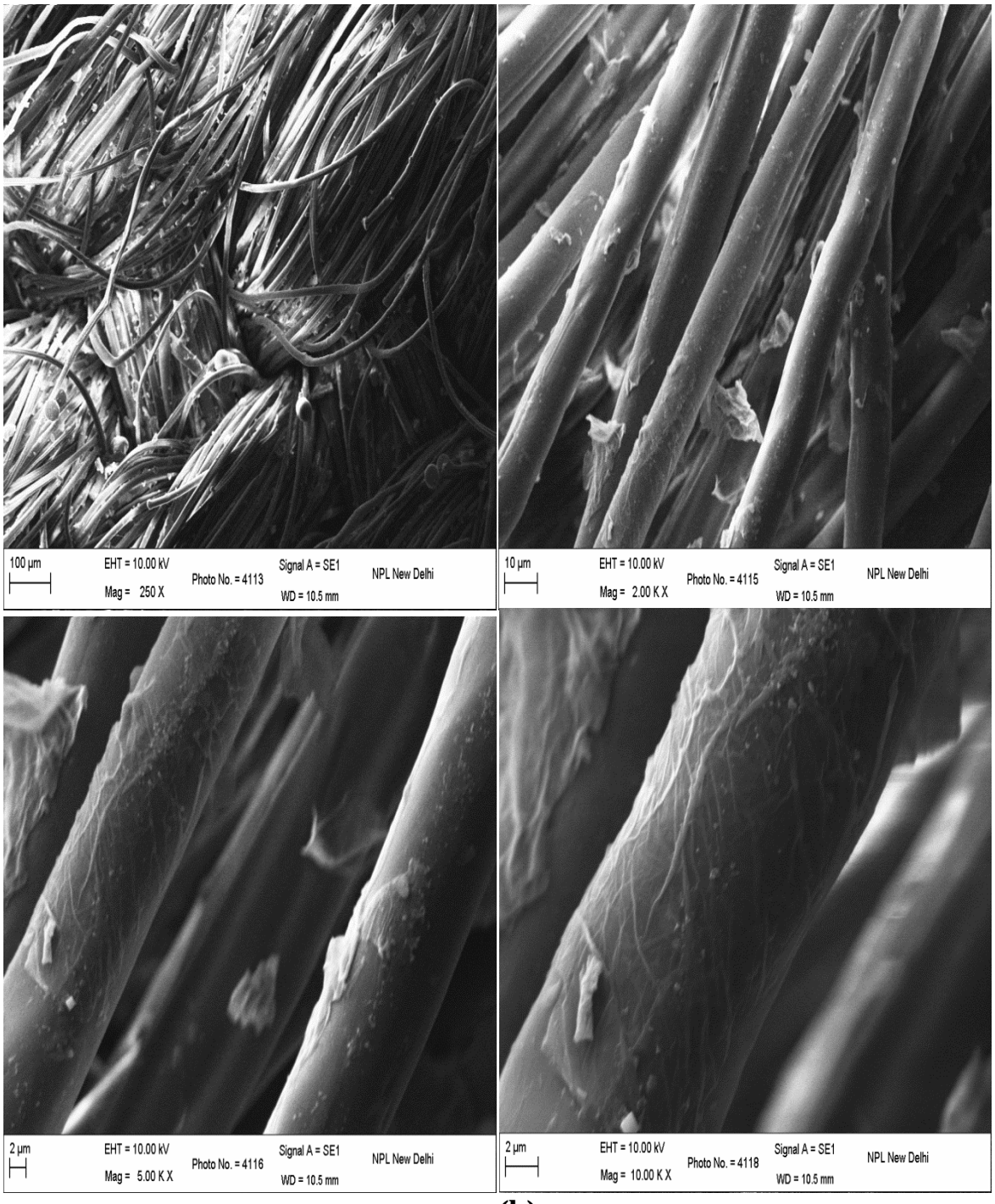
100 µm
EHT = 10.00 kV
Mag = 250 X
Photo No. = 4113
Signal A = SE1
WD = 10.5 mm
NPL New Delhi
10 µm
EHT = 10.00 kV
Mag = 2.00 K X
Photo No. = 4115
Signal A = SE1
WD = 10.5 mm
NPL New Delhi
2 µm
EHT = 10.00 kV
Mag = 5.00 K X
Photo No. = 4116
Signal A = SE1
WD = 10.5 mm
NPL New Delhi
2 µm
EHT = 10.00 kV
Mag = 10.00 K X
Photo No. = 4118
Signal A = SE1
WD = 10.5 mm
NPL New Delhi

(b)

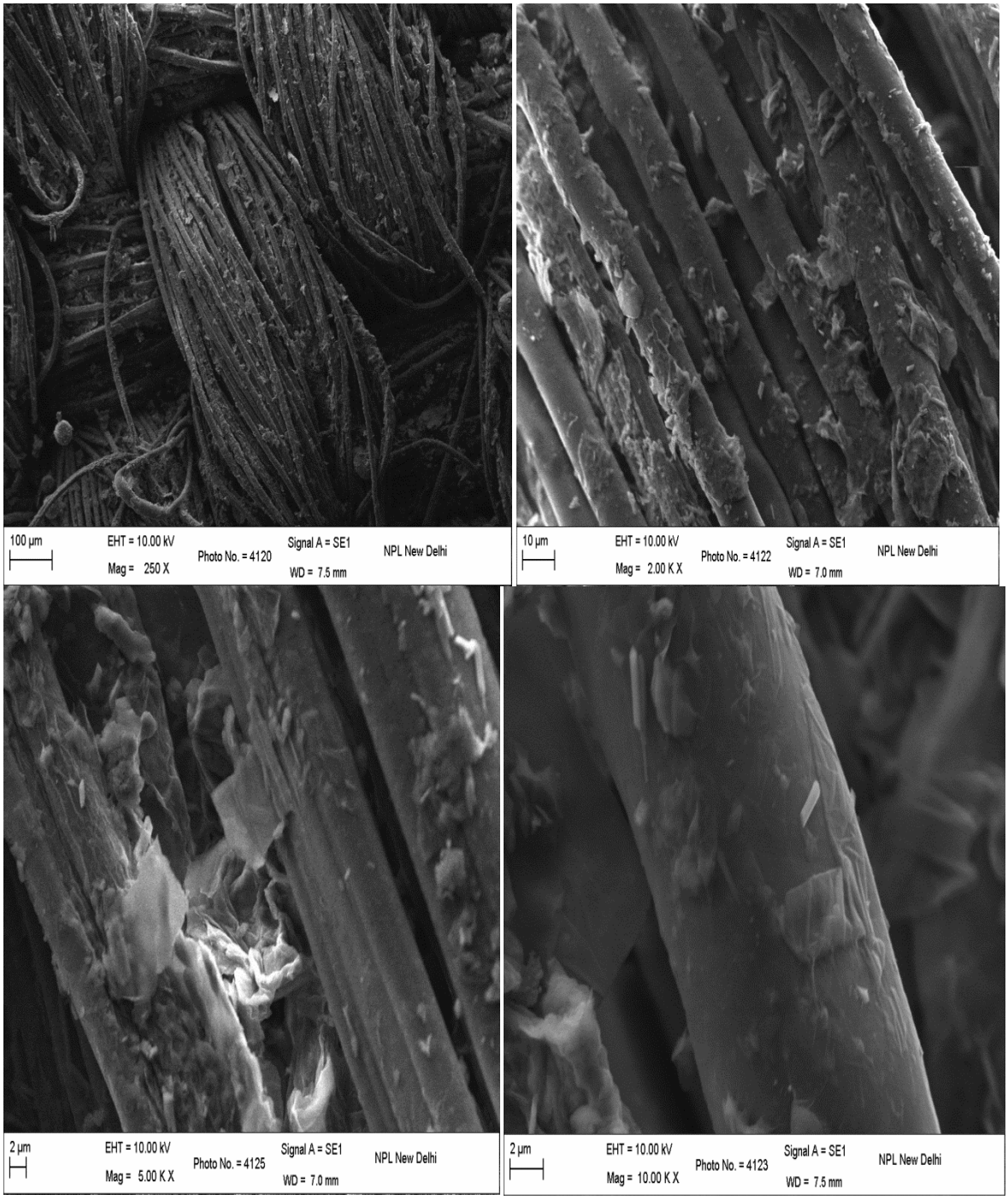
100 µm
EHT = 10.00 kV
Mag = 250 X
Photo No. = 4120
Signal A = SE1
WD = 7.5 mm
NPL New Delhi
10 µm
EHT = 10.00 kV
Mag = 2.00 K X
Photo No. = 4122
Signal A = SE1
WD = 7.0 mm
NPL New Delhi
2 µm
EHT = 10.00 kV
Mag = 5.00 K X
Photo No. = 4125
Signal A = SE1
WD = 7.0 mm
NPL New Delhi
2 µm
EHT = 10.00 kV
Mag = 10.00 K X
Photo No. = 4123
Signal A = SE1
WD = 7.5 mm
NPL New Delhi

(c)

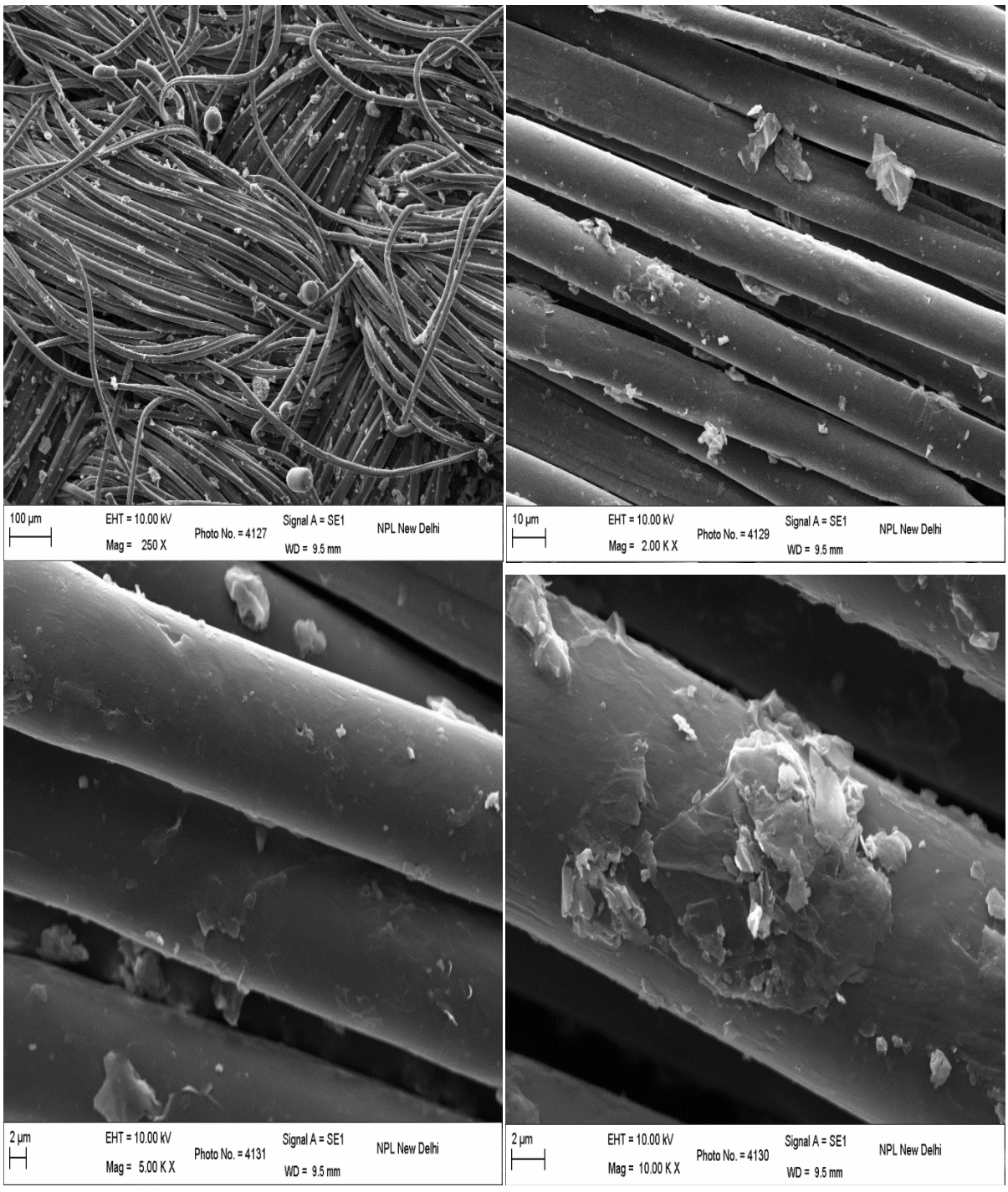
100 µm
EHT = 10.00 kV
Mag = 250 X
Photo No. = 4127
Signal A = SE1
WD = 9.5 mm
NPL New Delhi
10 µm
EHT = 10.00 kV
Mag = 2.00 K X
Photo No. = 4129
Signal A = SE1
WD = 9.5 mm
NPL New Delhi
2 µm
EHT = 10.00 kV
Mag = 5.00 K X
Photo No. = 4131
Signal A = SE1
WD = 9.5 mm
NPL New Delhi
2 µm
EHT = 10.00 kV
Mag = 10.00 K X
Photo No. = 4130
Signal A = SE1
WD = 9.5 mm
NPL New Delhi

(d)

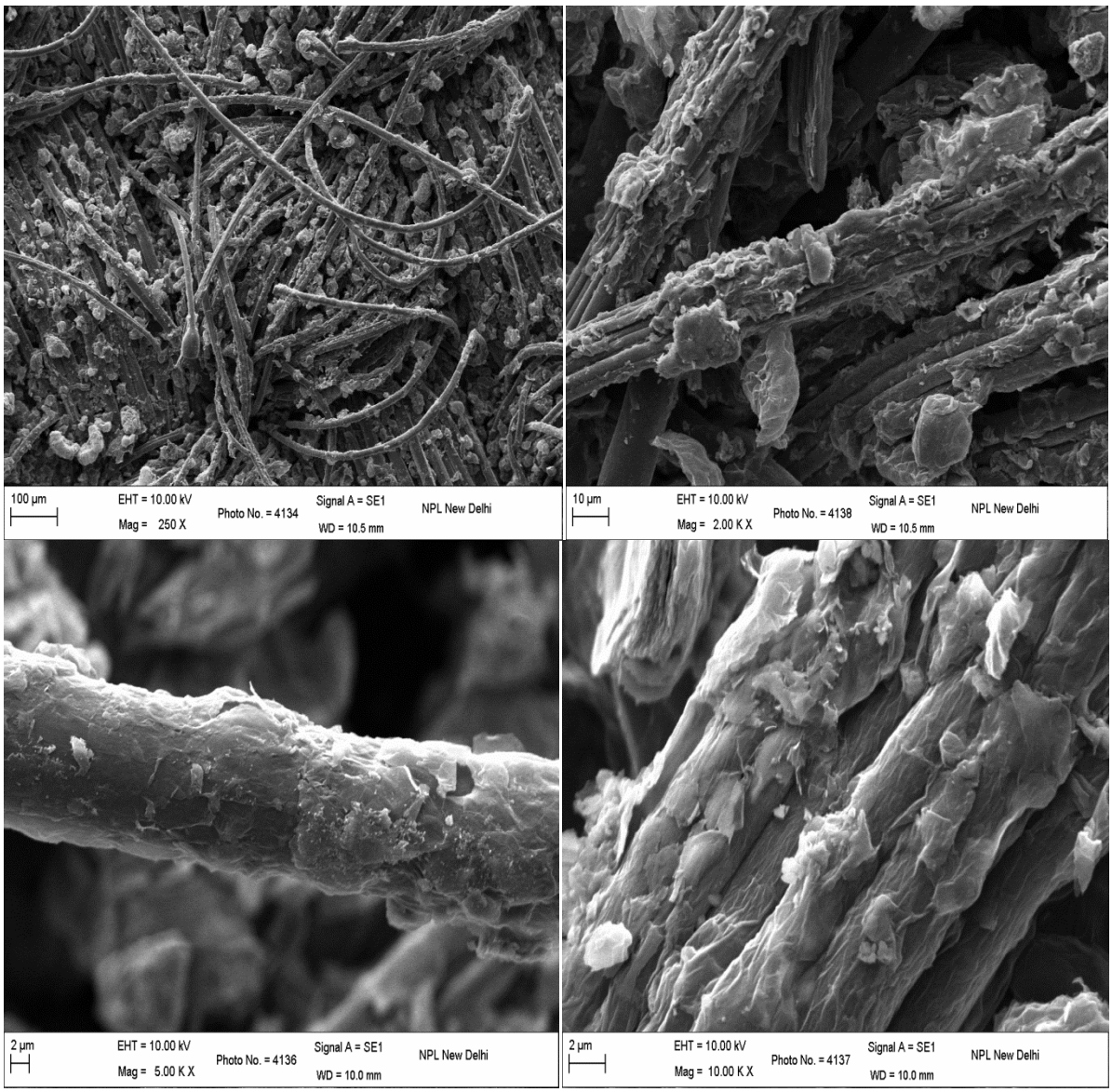

(e)

Fig 24: SEM images of (a) WF, (b) 1FGO, (c) 3FGO, (d) 1RVFGO, (e) 3RVFGO

4.8 X-RAY DIFFRACTION ANALYSIS OF FABRIC SAMPLES

Figure-25 shows XRD pattern of sample pure washed fabric (WF), 1FGO, 2FGO, 3FGO, 1RVFGO, 2RVFGO, 3RVFGO. XRD pattern of pure fabric shows three peaks at 2Θ= 17.0, 22.1, 25.5 degree that represent the characteristic peaks of cotton polyester fabric. In 1FGO with lowest loading level of GO, the characteristic peaks of GO are not observed as they are masked by dominant peaks of fabric substrate However, with the increase of GO loading level, the GO peak at $2\Theta = 10.1^{o}$ starts to appear Therefore, 2FGO and 3FGO fabrics show superimposed peaks of GO and cotton-polyester with progressive increase in intensity of GO peaks. In it important to point out that even after reduction, the graphene peak around 24^{0} cannot be observed as it was lies in the same region as the characteristic peaks of the fabric and therefore got suppressed for the sample 1RVFGO, 2RVFGO and 3RVFGO.

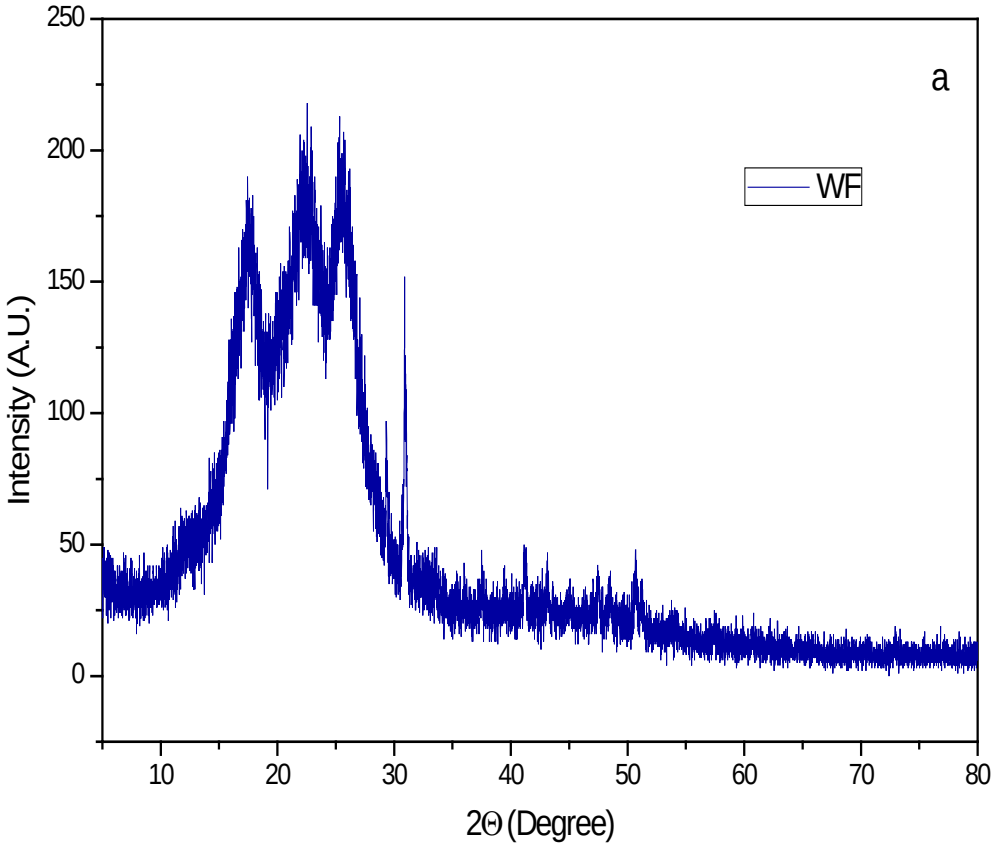

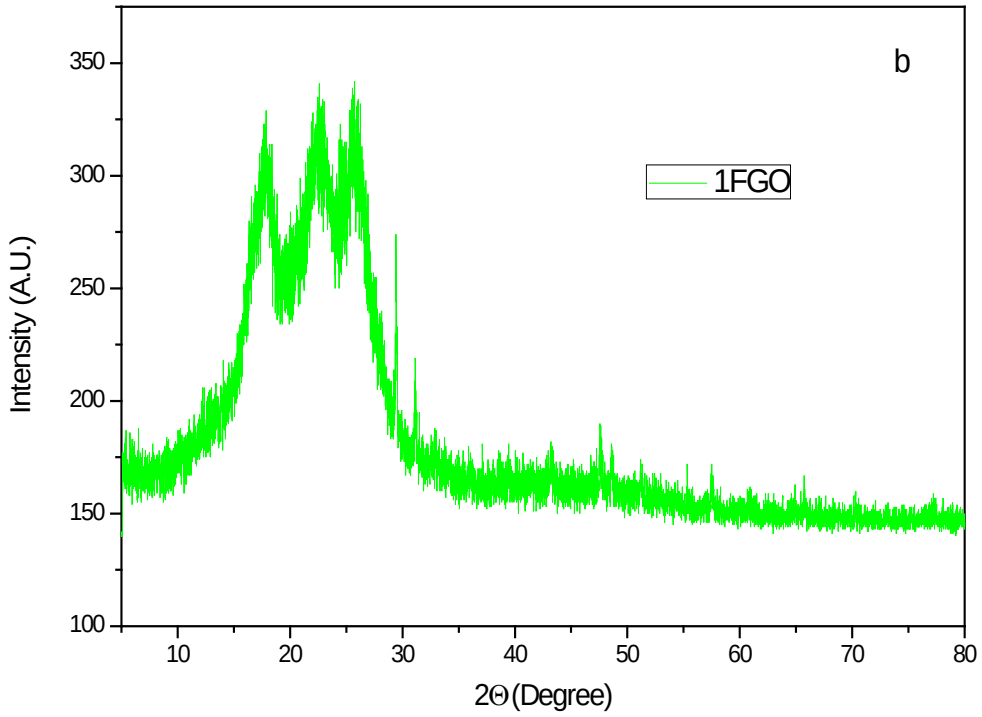
b
1FGO
Intensity (A.U.)
2Θ (Degree)
350
300
250
200
150
100
10
20
30
40
50
60
70
80

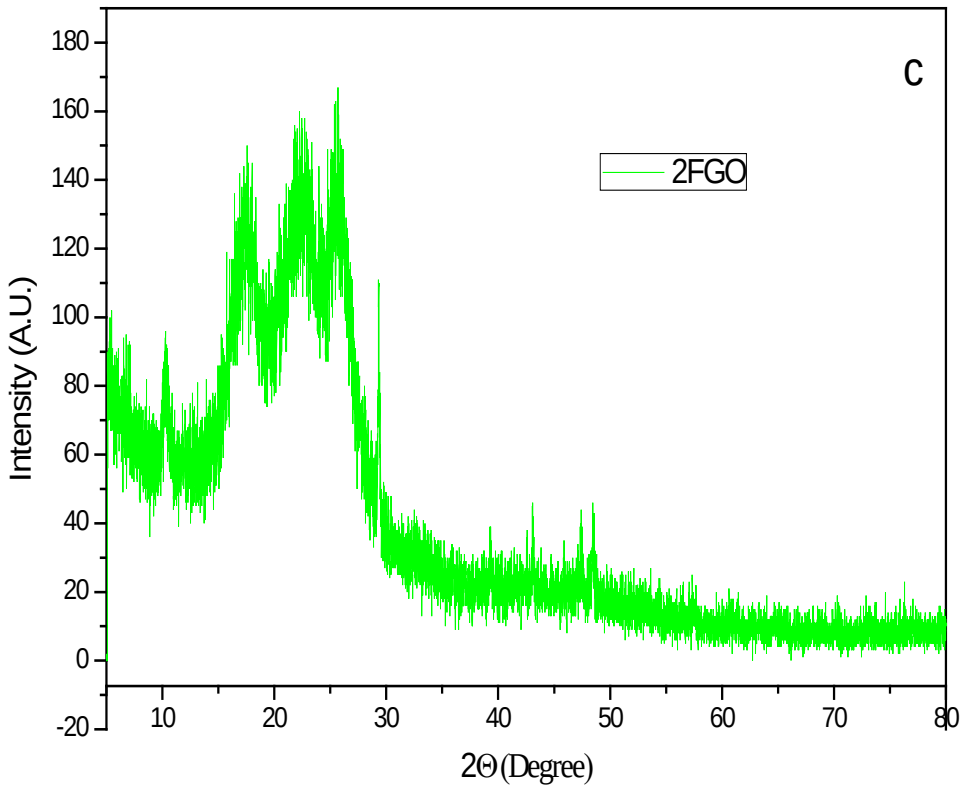
c
2FGO
Intensity (A.U.)
2Θ (Degree)
180
160
140
120
100
80
60
40
20
0
-20
10
20
30
40
50
60
70
80

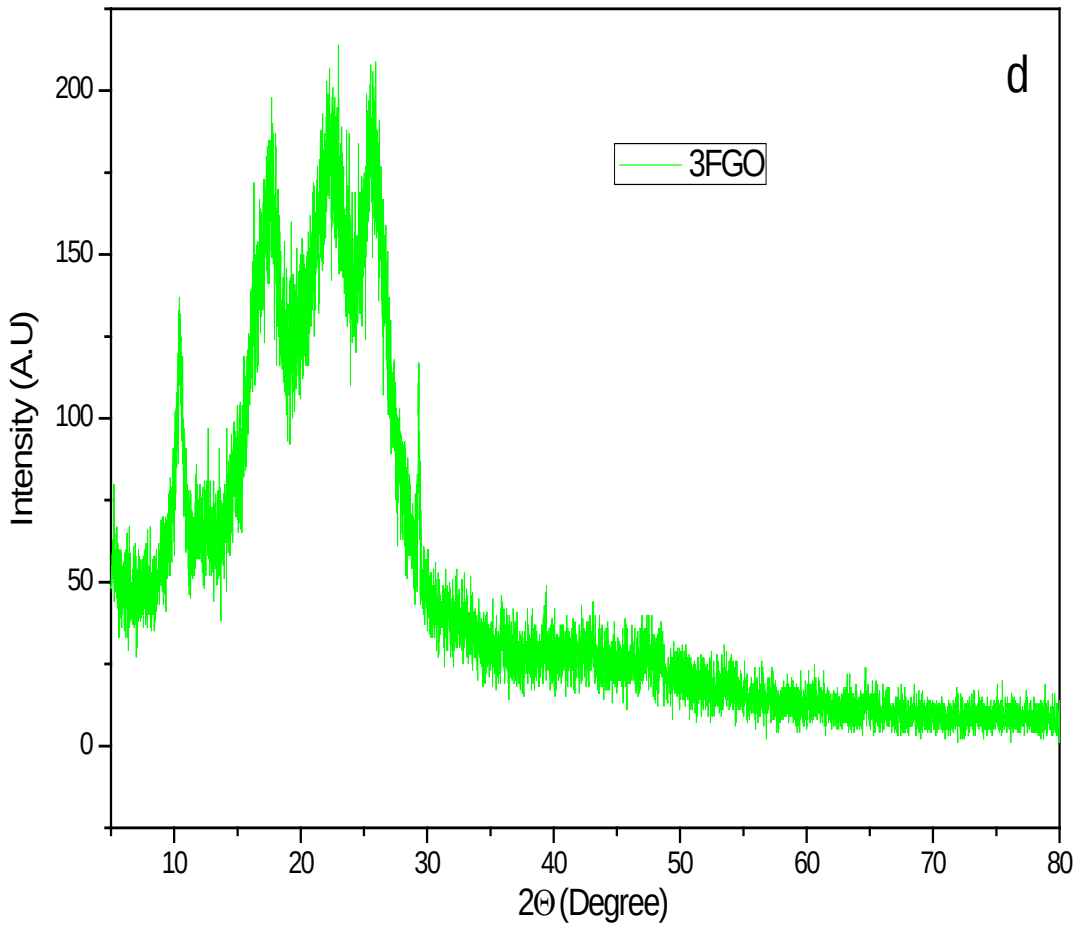
d
3FGO
Intensity (A.U)
2Θ (Degree)
0
50
100
150
200
10
20
30
40
50
60
70
80

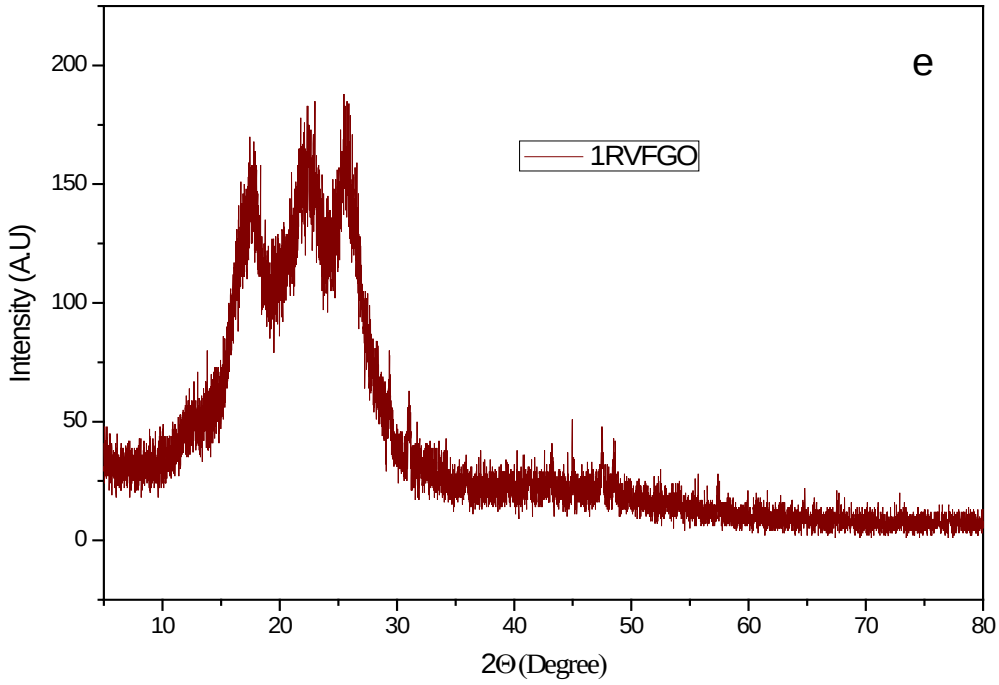
e
1RVFGO
Intensity (A.U)
2Θ (Degree)
0
50
100
150
200
10
20
30
40
50
60
70
80

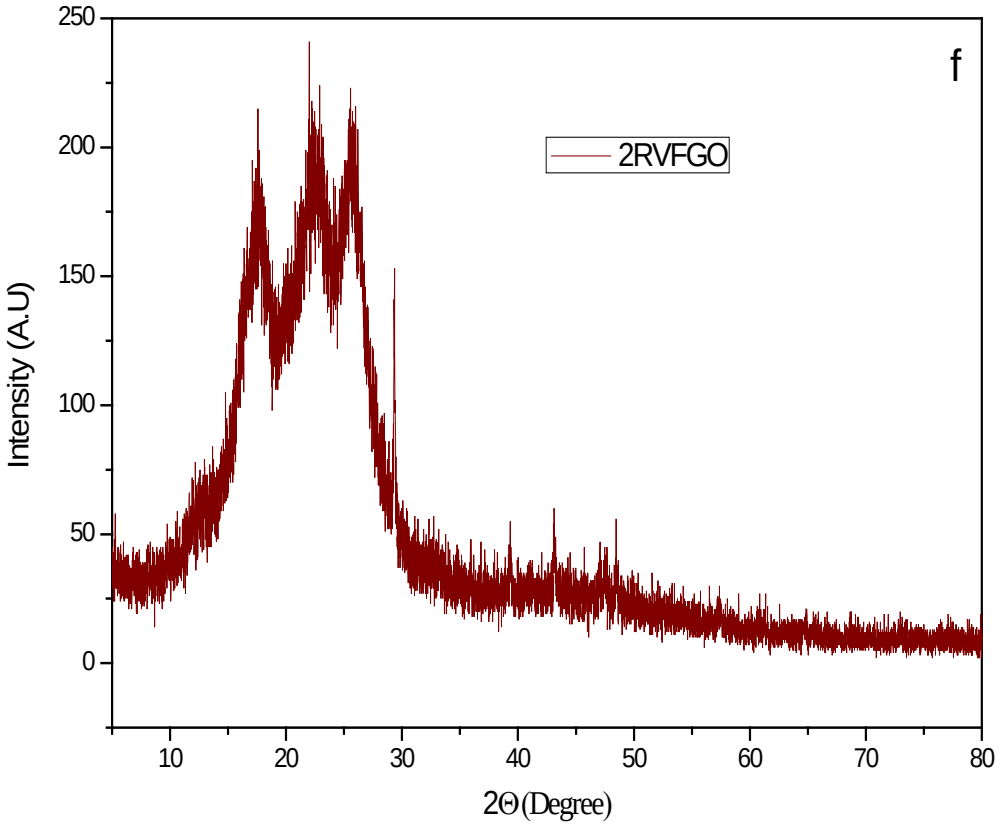
f
2RVFGO
Intensity (A.U)
2Θ (Degree)
0
50
100
150
200
250
10
20
30
40
50
60
70
80

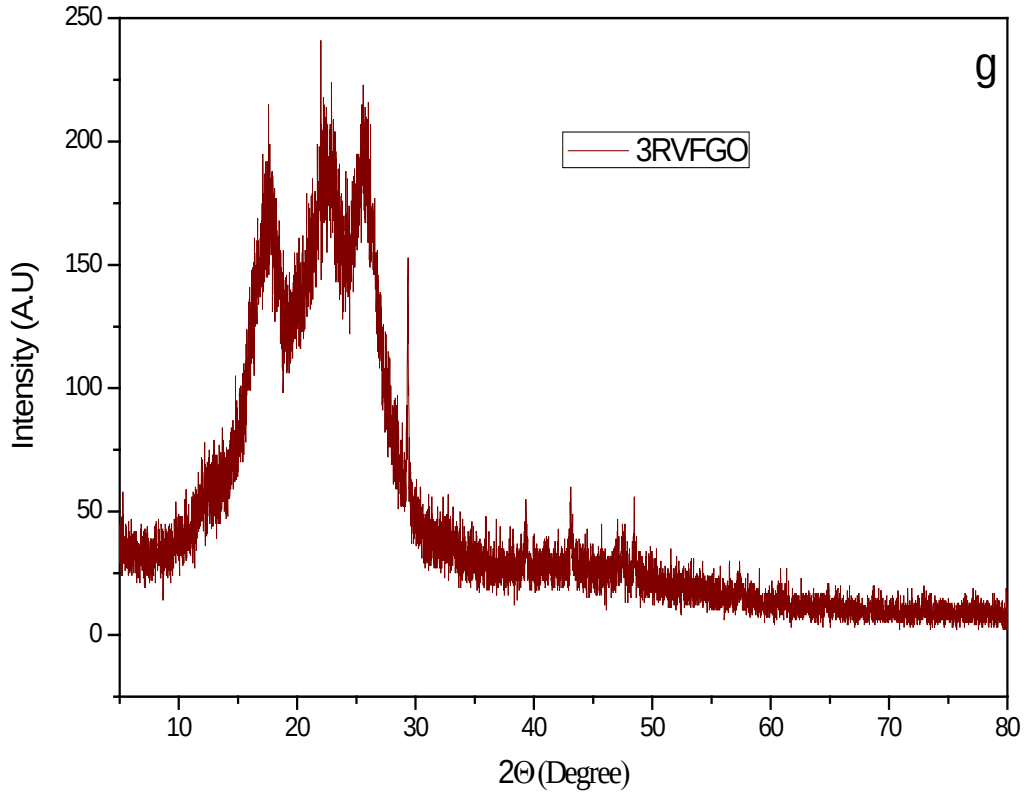

Fig 25: XRD pattern of pure fabric (a), GO coated fabric (b,c,d), Graphene coated fabric(e,f,g)

4.9 THERMO GRAVIMETRIC ANALYSIS OF FABRIC SAMPLES

Fig. 26, Table: 3 shows the TG traces of pure fabric, GO coated fabric (2FGO) and reduced GO coated fabric (2RVFGO). It can be seen that all the samples are quite stable up to temperature 260^0Cand show two step degradation. The pure fabric was stable upto 260 after which it abruptly loses approximately 81 % mass in two steps [i.e. ~14 (between 260-370) and ~67 (370-490)] that can be ascribed to degradation of polymeric backbone of the fibre constituents. In comparison, the GO and RGO coated fabrics show observable change in position of loss steps and related mass losses along with amount of residue remaining at 800^0 C. The GO coated fabric shows mass losses of 13% and 65% in the temperature range 260-355^0C and 355-490^0C respectively with char residue (at 800^0 C) of 13 %. In contrast, RGO coated fabric display mass losses of 8% and 70% in the temperature range 260-330^0C and 330-490^0C respectively with char residue (at 800^0 C) of 14 %. It is important to note that char residue is in the order pure fabric> FGO>RVFGO which can be ascribed to the highest thermal stability of RGO followed by GO and pure fabric. Same trend observed with 3FGO

and 3RVFGO with more char residue at 800^0C which is well agreement with loading percentage of GO, and RGO (Table 3, Figure 26).

Table 3: TGA analysis of Fabric samples

Sample designation	% mass loss		% char yield at 800 °C
	260-370 °C	370-490 °C	
WF	14	67	10
2FGO	13	65	13
2RVFGO	8	70	14

Sample designation	% mass loss		% char yield at 800 °C
	260-370 °C	370-490 °C	
WF	15	66	10
3FGO	13	68	12
3RVFGO	11	78	15

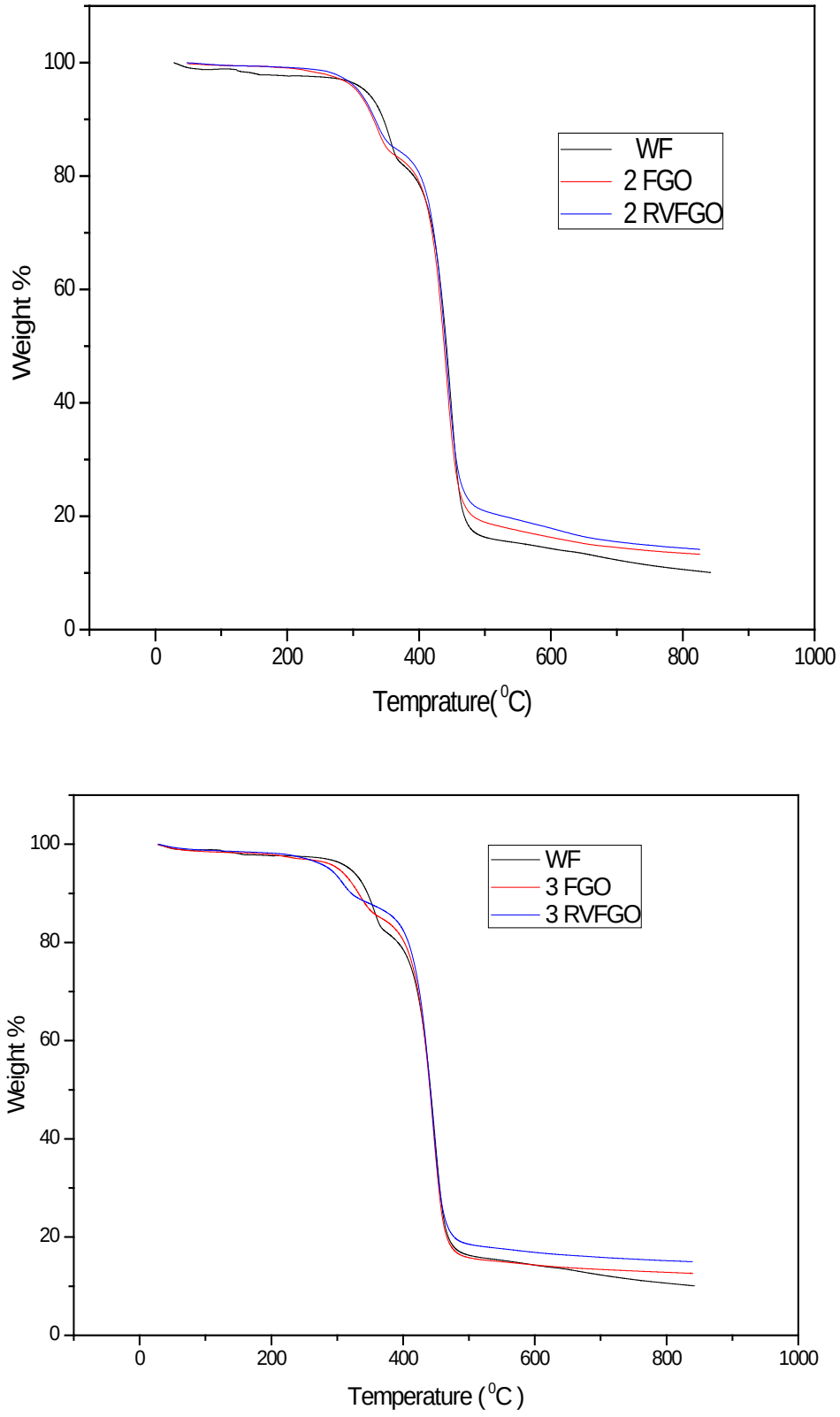

Fig 26: TGA result of fabric samples

4.10 CONTACT ANGLE MEASUREMENTS

The wetting properties of the fabrics were analyzed by measuring water droplet contact angle method. Contact angle of GO coated fabric and reduced GO coated fabric is given in the table 4 & 5, Figure 27. Pure cotton-polyester fabric shows the contact angle of 119.68. After coating of fabric with GO, the fabric showed a better wetting behaviour when contacted with water droplets. By increasing the GO coating on the fabric contact angle decreased to zero. Which shows improve hydrophilic nature of the GO coated fabric that can be attributed to the oxygenated functional groups present on the GO coating over fabric's surface. After reduction of GO coated fabric, wetting property of the fabric decreased due to the removal of oxygenated functional groups from the surface and enhancement of hydrophobic property.

Table 4: Contact Angle of GO Coated Fabric

Sample	Contact Angle
WF	**119.68 ± 5**
1FGO	**78.3 ± 5**
2FGO	**0.0 ± 5**
3FGO	**0.0 ±5**

Table 5: Contact angle of Graphene coated fabric

Sample	Contact Angle
1RVFGO	115.13 ± 5
2RVFGO	125.43 ± 5
3RVFGO	134.69 ± 5

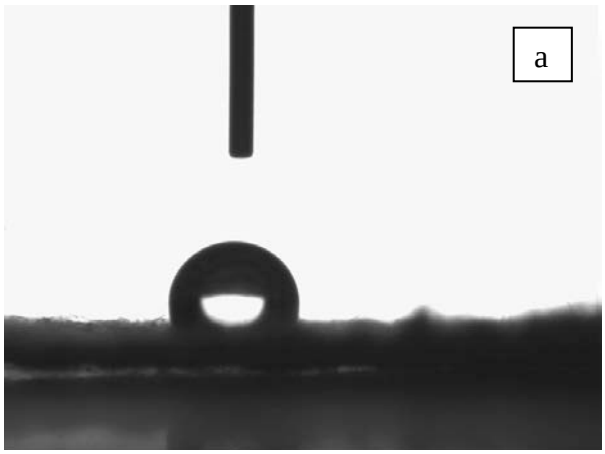

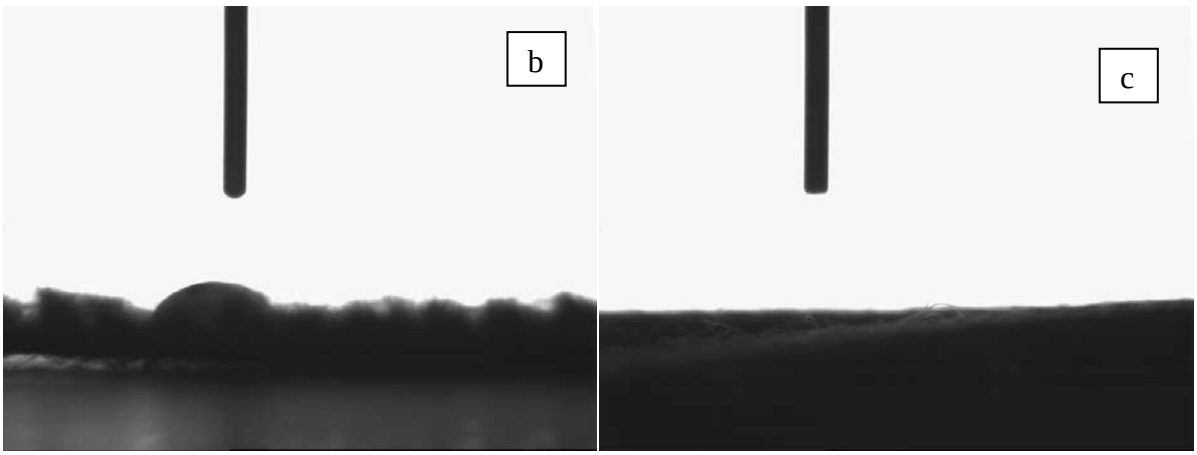

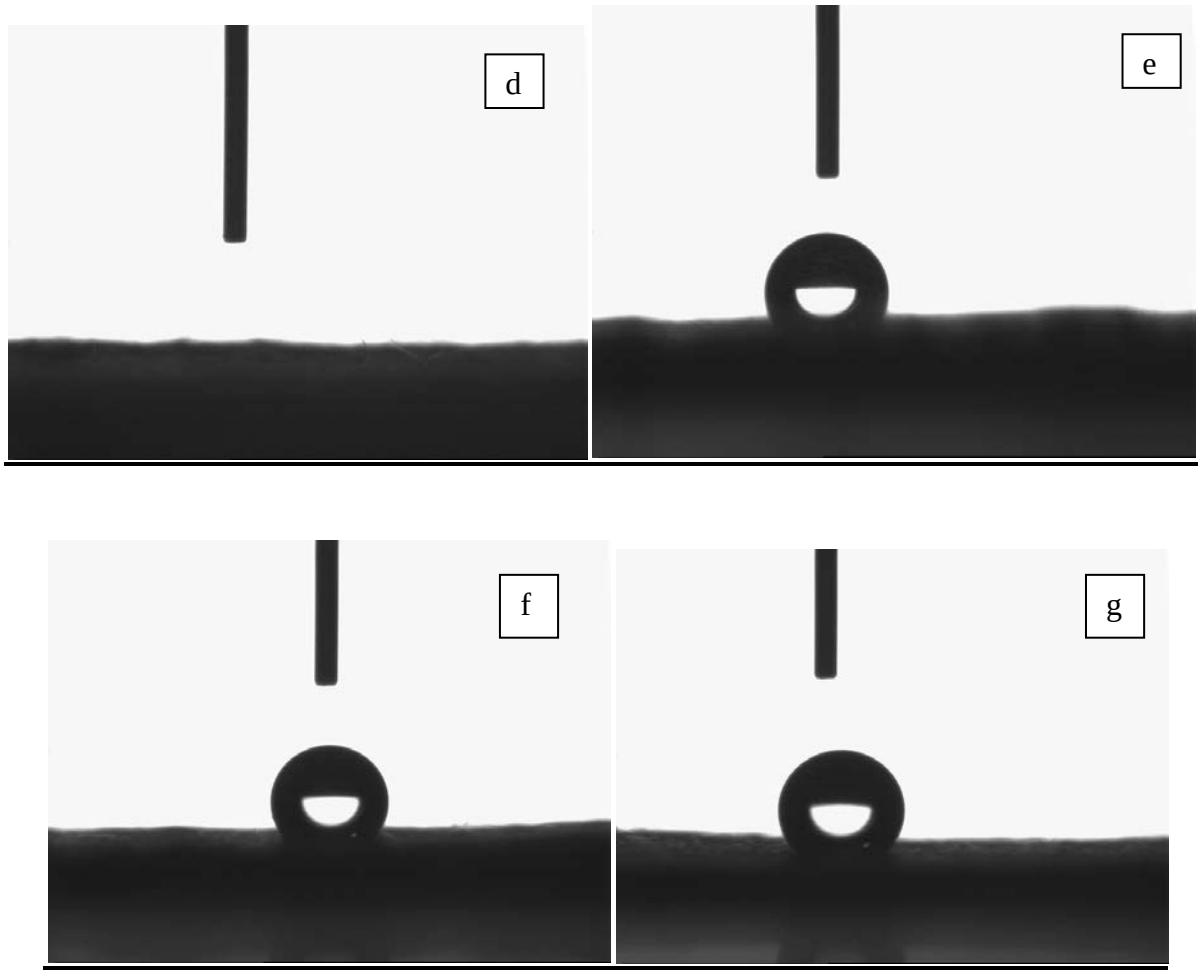

Fig 27: Contact angle results (a)WF, (b) 1FGO, (c)2FGO, (d)3FGO,(e)1RVFGO, (f)2RVFGO, (g)3RVFGO

4.11 MECHANICAL PROPERTIES

Textile performance of the modified cotton fabrics were evaluated in terms of mechanical properties viz. tensile strength, modulus, elongation at break etc. and the results are presented in Table 6. In comparison with the original cotton, tensile strength of the GO-coated fabric slightly increased this is due to the stacking of the mechanically strong GO layers on the surface of fabric leading to mechanical reinforcement. GO sheets present on the fabric surface also improve tensile modulus of the fabric. Decrease in the elongation at break of GO coated fabric was observed this may be due to the stiff nature of GO sheets. Variation of the mechanical property of GO coated fabric is shown in the Figure 28, 29 and 30.

Table 6: Tensile results of GO coated fabric

Sample	Tensile Strength (MPa)	Tensile Modulus (MPa)	Elongation at Break (mm)
WF	47.41	249	19.82
1FGO	58.73	313.06	24.07
2FGO	65.54	356.16	20.70
3FGO	68.29	467.42	17.63

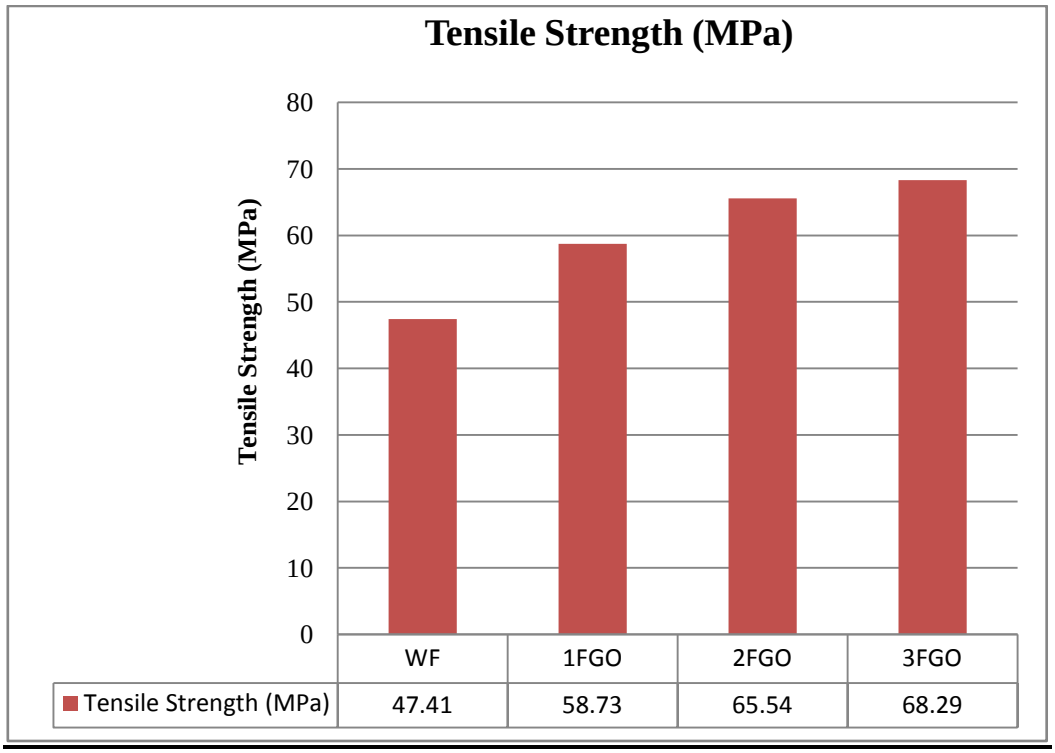

Fig 28: Tensile strength of GO coated fabric

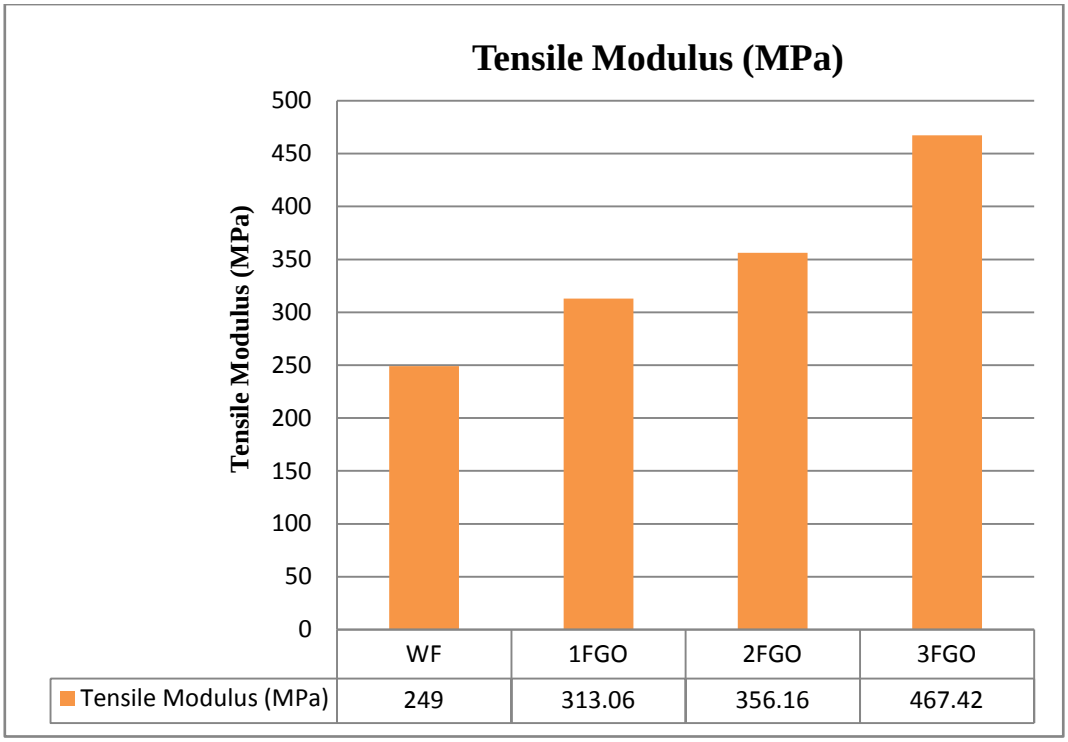

Fig 29: Tensile Modulus of GO coated fabric

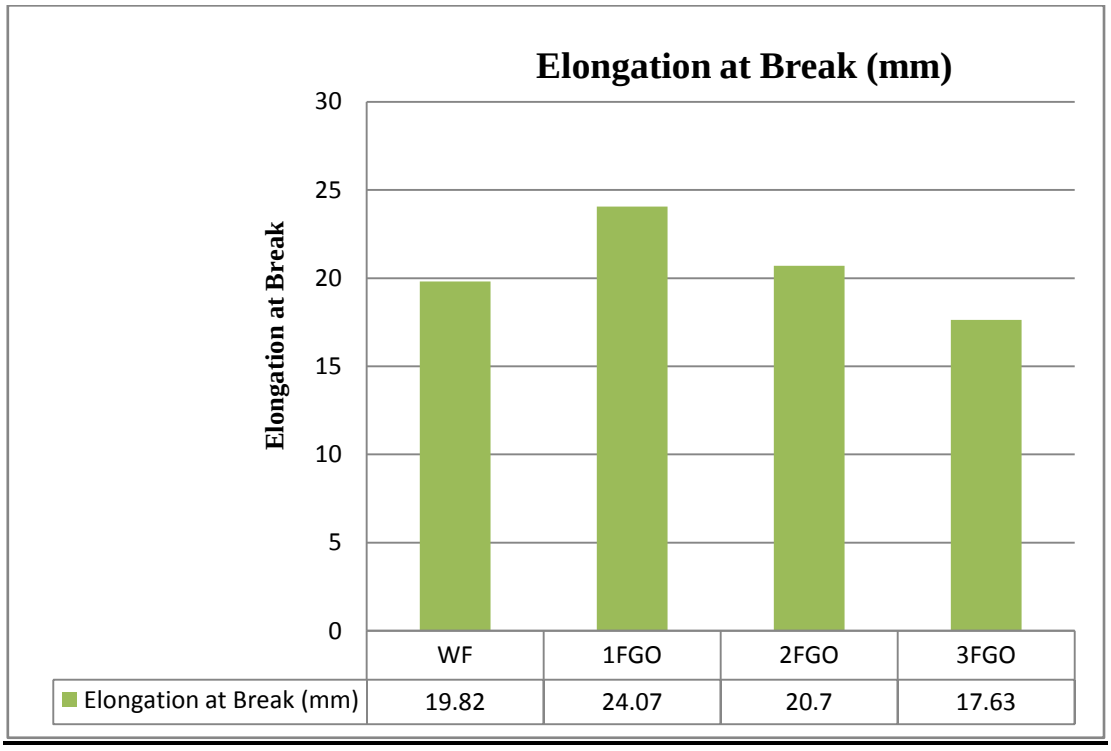

Fig 30: Elongation at break of GO coated fabric

4.12 RESISTANCE/CONDUCTIVITY MEASUREMENT

Since the electrical conductivity is best indicator of the extent to which the GO has been reduced to graphene, the surface resistivity of the fabrics was measured by two probe method and the obtained data are presented in Table 7-8. Since GO lacked an extended Π conjugated orbital system; the GO–cotton fabric was not electro conductive as their resistance are in GΩ range. After reduction treatment, the surface resistance of the GO–cotton samples was reduced, indicating partial restoration of conjugation of graphene sheets present on the surface. In particular, the electrical conductivity increased by approximately six orders of magnitude as graphene loading increases from 2.18 % to 3.75%. It is important to note that 1RVFGO lies at the borderline (<10^9 ohms) whereas 2RVFGO (with resistance of few hundred MΩ) display sufficient conductivity to show antistatic action and continuous dissipation of any static charges. Further, the highest loading sample display the resistance value of several KΩ and expected to display EMI shielding action especially in thick samples.

Table 7: Resistance/Conductivity of GO coated fabric

Sample	Resistance Value
1FGO	**52.0 GΩ**
2FGO	**4.0-10.0 GΩ**
3FGO	**2.2-3.6 GΩ**

Table 8: Resistance/Conductivity of graphene coated fabric

Sample	Resistance Value
1RVFGO	**0.28-0.4 GΩ**
2RVFGO	**0.23-33 MΩ**
3RVFGO	**76-95 KΩ**

4.13 EMI SHIELDING EFFECTIVENESS MEASUREMENT

Fabric was inserted in between source and antenna and the transmitted power was recorded from the detector. Shielding values were taken on shields made by single layer, double layer and triple layers of coated fabrics. Since the shielding effect depends on the conductivity as well as thickness, a definite trend was observed in the EMI measurements. It was observed that for a single layer of fabric, shielding effectiveness increases from -2.31 dB for 1RVFGO to -5.89 dB for 3RVFGO which is in agreement with decrease in sample resistance with increased loading of RGO. In addition, for any sample, shielding effectiveness increases (e.g. -2.31 dB to -5.48 dB for 1RVFGO and -5.89 dB to -8.90 dB for 3RVFGO) with increase in number of layers that can be attributed to thickness dependence of absorption as well as multiple scattering from various interfaces.

Table 9: EMI shielding effectiveness of graphene coated fabric

Sample-1RVFGO **Initial Power = 0.955 mW**		
No. of Layers	**Transmitted Power (mW)**	**Shielding Effectiveness (dB)**
Single Layer	0.56	-2.31
Double Layer	0.36	-4.23
Triple Layer	0.27	-5.48
S**ample- 2RVFGO** **Initial power = 0.933 mW**		
Single Layer	0.42	-3.46
Double Layer	0.28	-5.22
Triple Layer	0.18	-7.14
Sample-3RVFGO **Initial power = 0.933 mW**		
Single Layer	0.24	-5.89
Double Layer	0.16	-7.65
Triple Layer	0.12	-8.90

Nevertheless, the shielding effectiveness value of -8.9 dB for triple layer shield of 3RVFGO represents rather a very low attenuation. Therefore, attempt was made to further reduce the resistance of sample 3RVFGO by layer by layer deposition technique with GO dispersion followed by hydrazine hydrate reduction to achieve graphene loading of 7.1% and the sample was termed as HRVFGO. It was observed that as resistance decreased to 350 Ω, shielding effectiveness increases from -8.71dB to -26.67 dB for single layer to triple layer shield. It is important to point out that even a double layer shielding gives shielding effectiveness of ~ -20 dB (blocking of 99% of incident electromagnetic power) which suggest the suitability of these multilayered shields for making large area and flexible microwave absorbers.

Table: 10 EMI shielding effectiveness with high graphene loaded fabric

Sample – HRVFGO **Initial Power = 1.16mW**		
No. of Layers	**Transmitted Power (µW)**	**Shielding Effectiveness (dB)**
Single Layer	156	-8.71
Double Layer	12	-19.85
Triple Layer	2.5	-26.67

CHAPTER 5

CONCLUSION

Graphite oxide has been successfully synthesised and coated on fabric sample by simple dip coating method followed by reduction to graphene coated fabric. It shows good adherence with the fabric surface and coating was stable. The loading of graphene on fabric was varied between 2-7 weight % and samples were found to suitable for efficient attenuation of electromagnetic radiations. Based on the measurement results, following conclusions can be made:

1. TGA trace of graphite and GO show thermal stability of Graphite and GO. Graphite remains quite stable from room temperature to 800^0C while GO shows thermal instability due to presence of oxygenated functional groups which is also evidence for Graphite oxidation to GO.
2. XRD, FTIR and Raman spectra of GO confirms chemical oxidation of graphite to GO.
3. HRTEM microscopy of dispersed GO revealed layered sheet structure of graphitic sheets which are characteristics of few layer graphene.
4. SEM images of GO and Graphene coated fabric shows proper coating of GO and graphene on fabric surface. Coating is stable which also confirms the strong bonding between fabric and GO, RGO functional groups.
5. From Contact angle measurement it is confirmed that GO coated fabric shows hydrophilic nature and upon reduction to graphene it becomes hydrophobic, which is an indirect evidence of reduction of GO to Graphene.
6. Mechanical testing of GO coated fabric improved in tensile strength and tensile modulus which can be ascribed to GO layers on fabric surface while elongation at break decrease that is due to stiffness of GO sheets.
7. TGA traces of pure fabric, GO coated and graphene coated fabric showed stability and char remained at 800^0C in order of RVFGO>FGO>Fabric which better confirms the presence of GO and RGO sheets on the surface of fabric.
8. Resistance measurement show that GO coated fabric have high resistance value in the range of G-ohms, which is due to the oxygenated functional groups present on the surfaces which are is responsible for its high resistance. However, the reduction of

GO coated fabric leads to orders of magnitude improvement in conductivity due to the removal of oxygenated groups from the surface and restoration of layered structure and conjugation in graphene. The resistance of 2.18% graphene loaded fabric lies in borderline for antistatic property and may be used as antistatic material.

9. A single layer shield made up of fabric with ~7 weight % RGO loading gives shielding effectiveness (at 101GHz) value of -8.71dB which increases to -26.67 dB for a triple layer Shield. This reflect >99% attenuation and demonstrate the suitability of these fabrics for making future microwave absorbers.

REFERENCES

[1] P. Saini *et al*. "Improved Electromagnetic Interference Shielding Response of Poly(aniline)-Coated Fabrics Containing Dielectric and Magnetic Nanoparticles", J. Phys. Chem. C, *116*, 13403, **2012.**

[2] D.D.L. Chung, "Electromagnetic interference shielding effectiveness of carbon Materials", Carbon *39*, 279, **2001**.

[3] P. Saini, V. Choudhary, "Electrostatic charge dissipation and electromagnetic interference shielding response of polyaniline based conducting fabric", Ind. J. Pure and Appl. Phys., *51*, 112, **2013**.

[4] G. C. Marjanovic, "Recent advances in polyaniline composites with metals, metalloids and nonmetals", Syn. Met., *170*, 31, **2013**

[5] L. Vovchenko, *et al*. "Shielding coatings based on carbon–polymer composites", Surf. and Coating Tech., *211***,** 196, **2012**.

[6] J. Markarian, "New developments in antistatic and conductive additives", Plastics addi. and Comp, *10*, 22, **2008**

[7] W. S. Jou., *et al.* "The electromagnetic shielding effectiveness of carbon nanotubes polymer composites", J. of Alloy and Comp, *434-435*, 641, **2007**.

[8] N.V. Bhat, "Development of Conductive Cotton Fabrics for Heating Devices", J. Appl. Polym. Sci., *102*, 4690, **2006**.

[9] M. Shateri, and M. E. Yazdanshenas, "Preparation of superhydrophobic electroconductive graphene-coated cotton cellulose", Cellulose, *20*, 963, **2013**.

[10] H.H. Kuhn,et al. "Towards real application of conducting materials", Synthetic Metals, *71*, 2139, **1995**.

[11] C.Y. Lee, "Electromagnetic interference shielding by using conductive polypyrrole and metal compound coated on fabrics", Polym. Adv. Techn. *13*, 577, **2002**.

[12] J. Liang *et al*. "Electromagnetic interference shielding of graphene/epoxy composites", Carbon *47*, 922, **2009**.

[13] D. R. Dreyer *et al*. "From Conception to Realization: An Historical Account of Graphene and Some Perspectives for Its Future", Angew. Chem. Int. Ed. *49*, 9336, **2010.**

[14] Y. Zhu *et al.* "Graphene and Graphene Oxide: Synthesis, Properties, and Applications" Adv. Mater. *22*, 3906, **2010.**

[15] A.T. Collins, "The Optical and Electronic Properties of Semiconducting Diamond". Phil. Trans. Royal Soc. A, *342*, 233, **1993**.

[16] N. Deprez ,and D.S. McLachlan , "The analysis of the electrical conductivity of graphite conductivity of graphite powders during compaction", J. Phys. D: Appl. Phys., *21*,101, **1988**

[17] Fullerene encyclopedia britanica.

[18] M.F.L. De Volder, "Carbon Nanotubes: Present and Future Commercial Applications", Science, *339*, 535, **2013**.

[19] S. Iijima, "Carbon nanotubes: past, present, and future". Phys B.;*323*, 1, **2002**

[20] A.K. Geim, "Graphene prehistory", Phys. Scr.,*T146* , 014003, **2012**

[21] A.K. Geim and K. S. Novoselov, "The rise of graphene", Nature Materials, *6*, 183, **2007**.

[22] W. Choi, "Synthesis of Graphene and Its Applications: A Review", Critical Reviews in Solid State and Materials Sciences, *35*, 52, **2010**.

[23] R.S. Edwards, and K.S. Coleman, "Graphene synthesis: relationship to applications", Nanoscale, *5*, 38, **2013**.

[24] P. Avouris and C. Dimitrakopoulos, "Graphene: synthesis and applications ", Mat. Today, *15*, 86, **2012.**

[25] E. D. Grayfer *et al.* "Graphene: chemical approaches to the synthesis and modification", Russian Chem. Reviews *80*, 751, **2011**.

[26] C.Y. Su *et al.* "High-quality thin graphene films from fast electrochemical exfoliation, ACS Nano**,** *5*, 2332-2339, **2011**.

[27] W. Qian *et al*."Solvothermal-assisted exfoliation process to produce graphene with high yield and high quality", Nano Res. *2*, 706, **2009.**

[28] E.H.L. Falcao *et al*., "Microwave exfoliation of a graphite intercalation compound", Carbon *45*, 1364, **2007**.

[29] O.Y. Kwon *et al.*, "The preparation of exfoliated graphite by using microwave", J. Ind. Eng. Chem. *9*, 743, **2003**.

[30] D. V. Kosynkin *et al.* "Longitudinal unzipping of carbon nanotubes to form graphene nanoribbons", Nature *458*, 872, **2009**.

[31] Y.R. Kang, "Precise unzipping of flattened carbon nanotubes to regular graphene nanoribbons by acid cutting along the folded edges" J. Mater. Chem, *22*,16283, **2012**.

[32] X. Feng. *et al.* "Epitaxial growth of cubic silicon carbide on silicon by sublimation method", Optical Mat., *23*, 39, **2003**.

[33] C. Mattevi *et al.* "A review of chemical vapour deposition of graphene on copper" ,J.Mat. Chem, *21*, 3324, **2011.**

[34] B.C. Brodie, "On the atomic weight of graphite", Phil. Trans. Royal Soc. London, *149*, 249, **1859**.

[35] L. Staudenmaier, Verfahren zur Darstellung der Graphitsäure. Berichte der deutschen chemischen Gesellschaft, *31*, 1481, **1898**.

[36] L. Staudenmaier, Verfahren zur Darstellung der Graphitsäure. Berichte der deutschen chemischen Gesellschaft, *32*, 1394, **1899**.

[37] W.S. Hummers, and R.E. Offeman, "Preparation of Graphitic Oxide", J. Amer. Chem. Soc., *80*, 1339, **1958**.

[38] C. Hannes *et al.* "Functionalized Single Graphene Sheets Derived from Splitting Graphite Oxide " J. Phys. Chem. B, *110*, 8535, **2006**.

[39] D. Pandey *et al.* "Scanning probe microscopy study of exfoliated oxidized graphene sheets" Surface Science *602*, 1607, **2008**.

[40] M.J. McAllister, *et al.* "Single sheet functionalized graphene by oxidation and thermal expansion of graphite", Chem. Mater. *19*, 4396, **2007**.

[41] Y. Zhu *et al.*, "Microwave assisted exfoliation and reduction of graphite oxide for ultracapacitors", Carbon *48*, 2118, **2010**.

[42] S. Stankovich *et al.*, "Synthesis of graphene-based nanosheets via chemical reduction of exfoliated graphite oxide", Carbon *45*, 1558, **2007**.

[43] M. Periasamy, and M. Thirumalaikumar, “Methods of enhancement of reactivity and selectivity of sodium borohydride for applications in organic synthesis”, J. Organo Metallic Chem, *609*, 137, **2000**.

[44] M.J. F.-Merino *et al*. “Vitamin C is an ideal substitute for hydrazine in the reduction of graphene oxide suspensions”, J. Phys. Chem. C, *114*, 6426, **2010.**

[45] V. Singh *et al*., “Graphene based materials: Past, present and future”, Prog. Mater. Sci., *56*, 1178, **2011**.

[46] E. Y. Choi, “Noncovalent functionalization of graphene with end-functional polymers”, J.Mater. Chem., *20*, 1907, **2010**.

[47] Z. Wen, “Crumpled nitrogen doped graphene nanosheets with ultrahigh pore volume for high performance supercapacitor”, Adv. Mater, *24*, 5610, **2012**.

****